Progress in Oceanography 175 (2019) 309–327

Contents lists available at ScienceDirect

Progress in Oceanography

journal homepage: www.elsevier.com/locate/pocean

# Fine scale physical-biological interactions during a shift from relaxation to upwelling with a focus on *Dinophysis acuminata* and its potential ciliate prey

Patricio A. Díaz[a,b,*], Manuel Ruiz-Villarreal[c], Beatriz Mouriño-Carballido[d], Concepción Fernández-Pena[c], Pilar Riobó[e], Beatriz Reguera[a]

[a] Instituto Español de Oceanografía (IEO), Centro Oceanográfico de Vigo, Subida a Radio Faro 50, 36390 Vigo, Spain
[b] Centro i~mar & CeBiB, Universidad de Los Lagos, Casilla 557, Puerto Montt, Chile
[c] Instituto Español de Oceanografía (IEO), Centro Oceanográfico de A Coruña, Paseo Marítimo Alcalde Francisco Vázquez 10, 15001 A Coruña, Spain
[d] Departamento de Ecología y Biología Animal, Universidad de Vigo, Campus Universitario As Lagoas-Marcosende, E-36310 Vigo, Spain
[e] Instituto de Investigaciones Marinas (IIM-CSIC), Eduardo Cabello 6, 32208 Vigo, Spain

ARTICLE INFO

*Keywords:*
*Dinophysis acuminata*
Potential ciliate prey
Physical-biological interactions
Fine scale structure
Turbulence, division rates
Circadian variability, Galician Rías

ABSTRACT

Wind reversals and quick transitions from relaxation to upwelling in coastal areas cause major changes in water column structure, phytoplankton distribution and dominance, and rates of physiological processes. The cruise "*ASIMUTH-Rías*" (17–21 June 2013) was carried out in the Galician Rías and adjacent shelf, at the time of a DSP outbreak, to study small-scale physical processes associated with late spring blooms of *D. acuminata* and accompanying microzooplanktonic ciliates with the overall objective of improving predictive models of their occurrence. The cruise coincided with the initiation of an upwelling pulse following relaxation and deepening of a previously formed thin layer of diatoms. A 36-h cell cycle study carried on 18–20 June showed the vertical excursions of the thin layer, mainly delimited by the 13.5–14 °C isotherms and turbulence levels ($\varepsilon$) of $10^{-8}$–$10^{-6}$ m$^2$ s$^{-3}$, as well as marked changes in phytoplankton composition (increased density and dominance of diatoms). There was no evidence of daily vertical migration of *D. acuminata,* which remained in the top layer during the cycle study, but the opposite was observed in the ciliate populations. *Dinophysis* and its potential prey (*Mesodinium* species) cell maxima overlapped after midday, when the ciliate moved to the surface, suggesting an "ambush" strategy of *Dinophysis* to catch prey. A remarkable decline (from 0.65 to 0.33 d$^{-1}$) in division rates ($\mu$) of *D. acuminata* was associated with increased turbulence ($\varepsilon < 10^{-4}$ m$^2$ s$^{-3}$) near the surface and a sharp drop of temperature (> 2°C in about 8 h). In contrast, high division rates ($\mu_{min} \sim 0.69$ d$^{-1}$) persisted at a mid-shelf station where environmental conditions below the mixed layer were more stable. The onset of upwelling pulses appears to have a double negative effect on the net growth of *Dinophysis* populations: a direct physical effect due to advective dispersion and an indirect effect, decreased division rates. The latter would be caused by the rapid cooling of the mixed layer, and the increased turbulence at the surface resulting in shear stress to the cells. The short-term impact of upwelling pulses (and the winds promoting it) on the physiology of *Dinophysis* and its ciliate prey, and the role of mid-shelf populations of *Dinophysis* as a relatively undisturbed reservoir for the inoculation of subsequent blooms are discussed.

## 1. Introduction

Low density ($10^2$–$10^4$ cells L$^{-1}$) populations, i.e. low biomass harmful algal blooms, of *Dinophysis acuminata,* producer of diarrhetic shellfish poisoning (DSP) toxins, are the main cause of endemic shellfish harvesting bans in the Galician Rías Baixas, Northwest Iberian Peninsula (Blanco et al., 2005; Reguera et al., 2014). These rías are located in the northern limit of the Canary Current-Iberian Peninsula upwelling system (Fig. 1A). Winds, which vary considerably at a variety of temporal scales related to atmospheric oscillations, are the main drivers of hydrodynamics in upwelling systems (GEOHAB, 2005). Upwelling in northwestern Iberia is seasonal. On an annual basis, variability results from the seasonal evolution of the Azores high and the Iceland low which determine the wind regime and the onset of an upwelling (spring-summer) and a downwelling season (autumn-winter), separated by transition periods in spring and autumn (Bakun and Nelson, 1991). Variations in the wind regime on a time scale of days, due to changes in the position and strength of the high-low pressure

* Corresponding author at: Centro i~mar & CeBiB, Universidad de Los Lagos, Casilla 557, Puerto Montt, Chile.
*E-mail address:* patricio.diaz@ulagos.cl (P.A. Díaz).

https://doi.org/10.1016/j.pocean.2019.04.009
Received 6 October 2017; Received in revised form 18 February 2019; Accepted 29 April 2019
Available online 29 April 2019

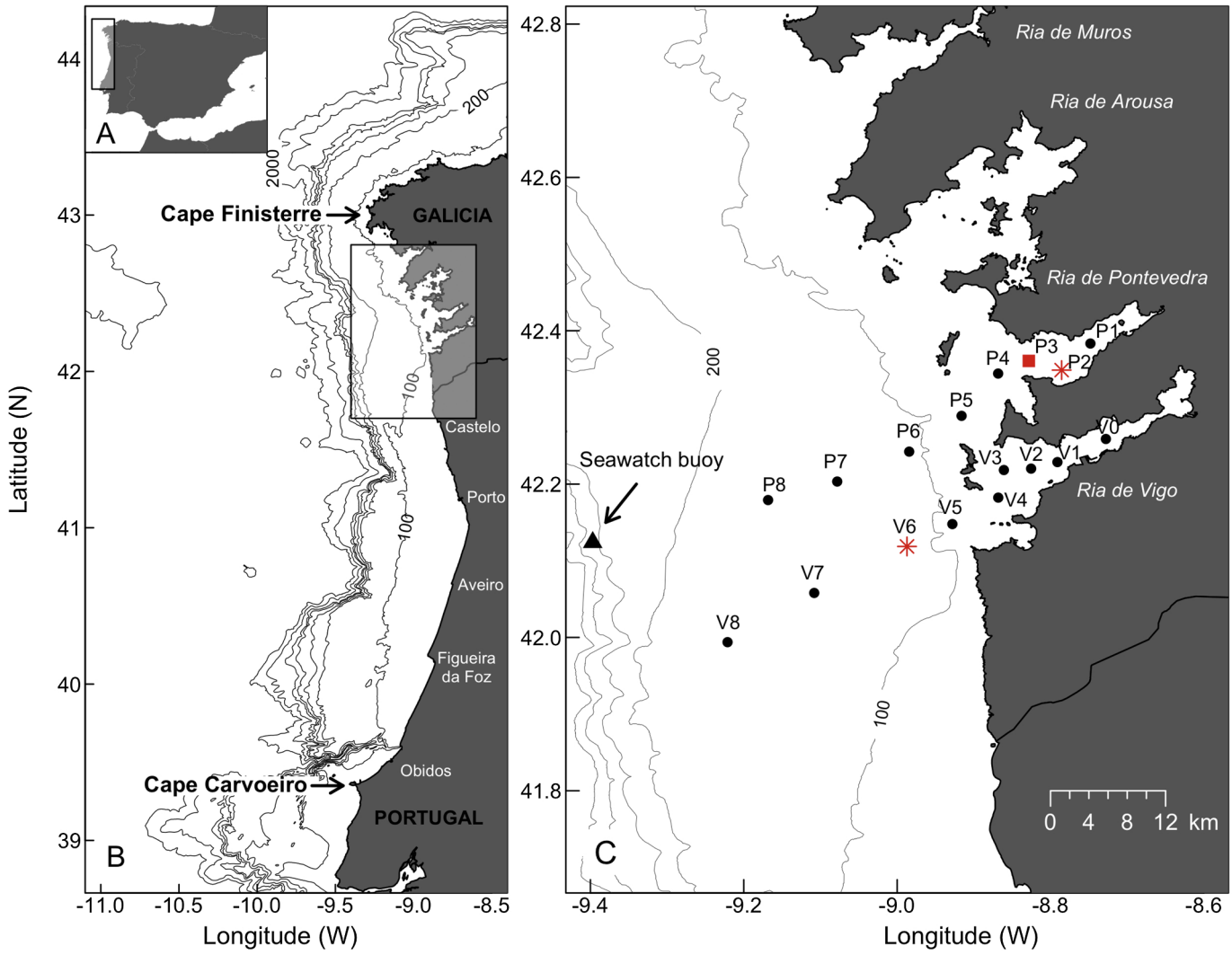


**Fig. 1.** Map of the study area showing the (A) Iberian Peninsula; (B) Northwest coast of Spain (the box delimits the Galician Rías Baixas) and the northern half of Portugal; (C) Map of the survey's sampling grid in the rías of Vigo (V0-V8) and Pontevedra (P1-P8). Red asterisks indicate the fixed station for the 36-h study (P2) and the shelf (100 m) station (V6) for estimates of vertical distribution of division rates; red square and black triangle, the mooring position of the ADCP and Cabo Silleiro Seawatch buoy, respectively. For interpretation of the references to colour in this figure legend, the reader is referred to the web version of this article.

systems, cause short-term hydrodynamic variability resulting in upwelling-downwelling cycles (Álvarez-Salgado et al., 2003; Gilcoto et al., 2017).

Turbulence plays a fundamental role in the structure and distribution of phytoplankton communities (Margalef, 1978; Smayda and Reynolds, 2001). Thus, diatoms dominate during mixing periods and dinoflagellates are more abundant during stable conditions (Margalef, 1978; Wyatt, 2014). Upwelling, an important source of turbulence in coastal systems, and wind stress controlling the upwelling-downwelling cycles, have been identified as the main drivers affecting the dominance of phytoplankton populations in the Galician Rías Baixas (Tilstone et al., 2000). In addition, short-term succession of these populations is modulated by semidiurnal and spring-neap tidal signals and its coupling to upwelling-downwelling events (Díaz et al., 2014).

Recently, Villamaña et al. (2017) used a microstructure turbulence profiler during spring and neap tides to characterize internal wave activity in the outer reaches of the Ría de Vigo. These authors showed that enhanced mixing, partially linked to intense internal wave activity during spring tides, in addition to the constructive interference of the shear associated with the upwelling and tidal currents (Fernández-Castro et al., 2018), caused a significant increase in nitrate diffusive fluxes. This nitrate supply could contribute to the dominance of large-sized diatoms during the upwelling favourable season (April-September) (Figueiras and Ríos, 1993; Moita and Silva, 2001). Nevertheless, turbulent mixing may also have disruptive effects on phytoplankton cells and in broad terms, dinoflagellates have been found to be more sensitive to turbulence than diatoms (Margalef et al., 1979; Thomas et al., 1995). Deleterious effects include changes in morphology (Berdalet and Estrada, 1995; Zirbel et al., 2000) and decline of cell division rates (Thomas and Gibson, 1990b; Thomas and Gibson, 1990a; Gibson and Thomas, 1995; Thomas et al., 1995).

The *D. acuminata* growth season, i.e. the time since a numerical increase in cell densities starts until the population declines to winter levels ($< 40$ cells $L^{-1}$), has been found to be tightly coupled to the local spring-summer upwelling season (Díaz et al., 2013; Velo-Suárez et al., 2014). Therefore, interactions between biological processes in *Dinophysis* populations (growth, vertical migration, toxin production) and quick changes of water-column structure associated with upwelling-downwelling cycles need to be scrutinized for the development of realistic prediction models (Ruiz-Villarreal et al., 2016).

For a given population, growth results from the positive balance between gains and losses and is governed by the fundamental equation:

$$dN(t)/dt = rN(t)$$

$$r = \mu + I_n - E_m - g - m$$

where $r$ is the net growth rate and $\mu$ the specific growth rate; $I_n$ and $E_m$ are immigration (advection, cyst germination) and emigration (dispersion, encystment), $g$ grazing and $m$, natural mortality rates. The *in situ* specific growth rate, $\mu$, estimates the potential for intrinsic division without the interference of losses due to grazing, mortality and physical dispersion (Carpenter and Chang, 1988). Therefore, estimates of $\mu$ help to identify oceanographic conditions that promote either active *in situ* division or accumulation resulting from physical/biological interactions (Reguera et al., 2003). Even more important for modeling purposes is to estimate $\mu_{max}$, i.e. the maximum potential division rate of the species under optimal conditions when resources are not limiting (Velo-Suárez et al., 2009). Models tend to use constant division rates, derived from laboratory experiments, for short (week) time-scale forecasts. Nevertheless, fast day-scale shifts in coastal wind-driven circulation, modulated by tides, may have dramatic effects on the net growth rate of a species population. The model of Carpenter and Chang (1988), based on the mitotic index approach (McDuff and Chisholm, 1982), has been successfully used to estimate *in situ* division rates ($\mu_{avg}$) of *Dinophysis* populations in different coastal environments (Chang and Carpenter, 1991; Garcés et al., 1997; Reguera et al., 2003; González-Gil et al., 2010; Aissaoui et al., 2014; Farrell et al., 2014). In most cases, an integrated or average value of $\mu$ ($\mu_{avg}$) for the whole water column, estimated from vertical net haul samples, was obtained. Nevertheless, in two cases when estimates of division rates at different depths $\mu_z$ were carried out, important vertical heterogeneities were observed (Velo-Suárez et al., 2009; Farrell et al., 2014).

*Dinophysis acuminata*, the target dinoflagellate species of this study, is an obligate kleptoplastidic mixotroph, i.e., it requires light, nutrients and plastids stolen from its ciliate prey for sustained growth (Park et al., 2006, Kim et al., 2008). To date, the phototrophic ciliate *Mesodinium rubrum*, which in turn requires cryptophyte prey belonging to the *Teleaulax/Plagioselmis/Geminigera* (TPG) clade, is the only known prey for *Dinophysis* species established in culture. This ciliate acts as a vector of cryptohyte plastids for the dinoflagellate (Park et al., 2006). The possibility of other plastid-retaining phototrophic ciliates being used as alternative prey to *Mesodinium* by *Dinophysis* species needs to be explored. For all these reasons, special attention was focused during the 36-h cycle study, on the distribution of *Mesodinium* and other plastid-bearing microzooplanktonic ciliates in relation to their potential predator, *Dinophysis*.

The cruise *ASIMUTH-Rías* was carried out in June 2013 in the Galician Rías of Vigo and Pontevedra and their adjacent shelf (Fig. 1B) to study small-scale physical-biological interactions in late spring blooms of *D. acuminata* during the upwelling season. These included the circadian variability of *Dinophysis* physiology (division rate, toxin content), daily vertical migration and biological interactions with their potential ciliate prey. Our main objective was to examine, with the support of high vertical resolution measurements of turbulence and current velocities, the short-term response of *D. acuminata* (distribution and physiology) and accompanying ciliate populations to rapid shifts from upwelling relaxation to new upwelling pulses in the Galician Rías Baixas.

## 2. Material and methods

This work was part of the cruise "*ASIMUTH-Rías* 2013", carried out on board R.V. *Ramón Margalef* from 17 to 21 June 2013 in the rías of Vigo and Pontevedra and their adjacent shelf. The cruise took place during a long-lasting DSP outbreak which led to shellfish harvesting closures from mid March to mid September in aquaculture sites in Ría de Pontevedra (Ruiz-Villarreal et al., 2016). Longitudinal transects from Ría de Pontevedra and Ria de Vigo (this one incomplete due to a ship breakdown on June 21) to the adjacent shelf were sampled on June 18 and 21 (Fig. 1C). In addition, a 36 h sampling, from 18 to 20 June, was carried out at a fixed station (P2, Bueu) from Ría de Pontevedra. This station is a hot-spot for diarrhetic shellfish poisoning (DSP) events, i.e. harvesting bans when toxins in shellfish meat exceed regulatory limits, in the Galician Rías Baixas (Blanco et al., 2013).

### 2.1. Meteorology and hydrology

Measurements of wind speed and direction were recorded from a buoy (Seawatch, Oceanor), belonging to the national port system (Puertos del Estado) network, deployed in Cabo Silleiro (42°7.89N − 9°23.49W) (Fig. 1C), a representative station for the study area. Additionally, high frequency (every 1 min) wind speed and direction data were obtained from the meteorological station located on board R/V *Ramón Margalef*. Estimates of Ekman's transport ($m^3\,s^{-1}\,km^{-1}$) according to Bakun (1973), every 6 h, were obtained from the Spanish Institute of Oceanography (IEO) (www.indicedeafloramiento.ieo.es) using geostrophic wind data from the buoy station. Tides and sea level measurements were taken with a tidal gauge from the IEO network deployed on Ría de Vigo harbour (http://indamar.ieo.es/). Differences in amplitude (< 10 cm) and tidal phase (1–2 min) in the tides semidiurnal component in both rías are negligible.

### 2.2. Microstructure turbulence profiler and ADCP measurements

Measurements of turbulence microstructure were obtained with a MSS (Prandke and Stips, 1998) profiler during the 36 h cell-cycle study at the fixed station (P2), and at the V5 shelf station (~100 m depth) on June 18 and 21. The profiler was equipped with 2 velocity microstructure shear sensors (type PSN06), a microstructure temperature sensor (FP07), a sensor to measure horizontal acceleration of the profiler and a high-precision CTD probe including a fluorescence sensor. The acquisition and processing of the shear data were performed with the commercial software SST-SDA (Standard Data Acquisition) and ProDat Sea & Sun Technology (www.sea-sun-tech.com/technology.html). The turbulent kinetic energy dissipation rate (ε) was estimated from the shear data following Fernández-Castro et al. (2014). In short, $\varepsilon$ was computed in 512 data point segments, with 50% overlap, from the shear variance, under the assumption of isotropic turbulence, using the following equation:

$$\varepsilon = 7.5\nu\left\langle\left(\frac{\partial u}{\partial z}\right)^2\right\rangle (\mathrm{W\ kg^{-1}}) \quad (1)$$

where $\nu$ is the kinematic viscosity of seawater, $\partial u = \partial z$ the vertical shear and $\langle\cdot\rangle$ represents the ensemble average. The shear variance was computed by integrating the shear power spectrum. The lower integration limit was determined considering the size of the bins, and set to 2 cpm. The upper cut-off wave number for the integration of the shear spectrum was set as the Kolmogoroff number ($k_c = \frac{1}{2\pi}\cdot(\varepsilon/\nu^3)^{1/4}$ cpm). An iterative procedure was applied to determine $k_c$. The maximum uppercut-off was not allowed to exceed 30 cpm to avoid the noisy part of the spectrum. Assuming a universal form of the shear spectrum, $\varepsilon$ was corrected for the loss of variance below and above the integration limits, using the polynomial functions reported by Prandke et al. (2000). Values of $\varepsilon$ were then averaged in 1 m bins. Peaks due to particle collisions were removed by comparing the dissipation rates computed simultaneously from the two shear sensors.

An RDI 600 Hz Sentinel Workhorse ADCP was moored, from June 14 to July 4, 2013, near the centre of the main navigation channel, between stations P2 and P3 (42° 21.41′ N; 08° 50.02′ W, Fig. 1C). Nominal depth at the mooring was 37 m. The ADCP was installed in a low drag float 2 m above the sea floor. Data were acquired through 3 min temporal ensembles and 1 m vertical bins. Raw data were post-processed with the IMOS ADCP toolbox and several quality control tests carried out —including tilting, echo intensity, correlation and side lobe

effects—to produce QC (quality controlled) current data at fixed depths above the sensor using tilt information.

### 2.3. Model simulations

Surface current fields were obtained from a Regional Ocean Model System (ROMS) configuration developed at IEO in the framework of the Iberian Margin Ocean Observatory project RAIA (Otero et al., 2013). This configuration was the same as that used by Ruiz-Villarreal et al. (2016) to investigate the effects of hydrodynamical conditions on toxic dinoflagellate blooms in Galicia. A high resolution 1.3 km grid centred in the Galician coast is nested in a 4 km grid of the Iberian shelf and slope. Realistic forcing includes tides, run-off from several rivers and atmospheric fluxes from the operational configuration of the Weather Research and Forecasting (WRF) mesoscale model run by Meteogalicia (www.meteogalicia.es). This forecast model configuration allows describing the response of the shelf and rias circulation to upwelling-downwelling pulses and its interplay with different physical forcings (Ruiz-Villarreal et al., 2016).

### 2.4. Field sampling

Data on *Dinophysis* cell densities in Ría de Pontevedra before and after the cruise were taken from weekly reports of phytoplankton distribution from the Galician Monitoring Programme at INTECMAR (www.intecmar.gal). In this programme, weekly plankton samples for quantitative analyses are collected with a dividable hose (tube-sampler) that samples the whole water column from 0 to 15 or 20 m, and immediately fixed on board with acidic Lugol's iodine solution.

During the survey, vertical profiles of temperature, salinity and fluorescence were obtained with a Sea-Bird SBE-25 conductivity-temperature-depth (CTD) profiler combined with a 12-bottle (2.5 L each) rosette (General Oceanics, USA).

Water samples for quantitative analysis of microphytoplankton (*Dinophysis*) and ciliates (every 2 h during the 36 h study), and *Dinophysis* division rate estimates (during the 36 h study and one vertical profile on a shelf station, see Section 2.7) were taken from 6 different depths selected after reading the CTD profile. These depths included surface (3 m), near the seabed, at the chlorophyll (chl) maximum and wherever any relevant discontinuity of physical properties was observed.

For *Dinophysis* studies, two kinds of samples were collected every 2 h from discrete depths: (1) unconcentrated seawater samples, immediately fixed with acidic Lugol's iodine solution, for quantitative analysis and (2) concentrated water samples (2.5 L), filtered through 20-μm nytex filters and resuspended in 50 mL of seawater fixed with formalin, to enumerate cell-cycle phases of *D. acuminata* (concentration factor = 50). Additional water samples of 250 mL, fixed with Lugol's solution, were taken for ciliate analyses.

Sampling for division rate estimates, during the cell-cycle study, was carried out every 2 h from 08:00 h to 02:00 h the next day (GMT), and every hour from 02:00 h to 08:00 h, which is the time window before dawn when phased division of *Dinophysis acuminata*. is observed, and proportion of dividing and recently-divided cells change very rapidly (Reguera et al., 2003).

For toxin analyses, vertical net hauls (one every 2 h) with a 20-μm mesh net were collected and passed through a 150-μm mesh to eliminate large microzooplanktonic organisms; an aliquot (~15 mL) from each haul sample, immediately fixed with acidic Lugol's solution, kept for cell counts; 200 mL of the hauled material filtered through Whatman (Whatman, Maidstone, England) GF/F fiberglass filters (47 mm Ø, 0.7-μm pore size), the filter and filtered material placed in a centrifuge tube and covered with analysis grade methanol; 50 mL of the filtered haul water collected for extracellular toxin analyses in a Falcon tube and all tubes placed in the vessel's deep-freeze and later transported in a portable fridge before final storage in the laboratory at −20 °C until analysis.

### 2.5. Toxin analyses

Toxin analyses by LC-HRMS were carried out in positive mode with a Thermo Scientific Dionex High-Speed LC coupled to an Exactive mass spectrometer equipped with an Orbitrap mass analyzer and a HESI-II probe for electrospray ionization.

Toxins were separated using an Aquity C18 column (2.1 × 150 mm, 3 μm particle size) maintained at 35 °C with a flow rate of 400 μL $min^{-1}$. The mobile phase consisted of 5 mM ammonium acetate pH 6.8 (A) and 95% MeOH: 5% mobile phase A (B). A linear gradient elution from 60% B to 100% B was run for 20 min. 100% B was held for 2 min before returning to the initial conditions of 60% B in 3 min. This percentage was held until min 30. Certified reference standard solutions of okadaic acid (OA), dinophysistoxin-2 (DTX2) and pectenotoxin-2 (PTX2) were purchased from the National Research Council (Canada). Calibration curves were obtained in triplicate for each toxin standard (variation coefficient 14%). The toxin concentration in sample extracts was quantified by comparing the area or the peaks obtained in the chromatograms with those of the certified reference material solutions.

### 2.6. Plankton analyses

For quantitative analyses of *Dinophysis* species, 25 mL of unconcentrated acidic Lugol's-fixed samples were left to sediment for 24 h and analysed under an inverted microscope (Nikon Eclipse 2000) using the method described in Utermöhl (1958). The whole surface of the chamber was scanned at a magnification of ×100, so that the detection limit was 40 cells $L^{-1}$. For quantitative analyses of ciliates, 100 mL of unconcentrated Lugol's-fixed samples were left to sediment for 48 h. Taxonomic classification was based on Lynn and Small (2002) criteria. Counts were performed at a 200× magnification under a Nikon Eclipse TE 300 inverted microscope according to Utermöhl (1958).

### 2.7. Estimates of division rates

To enumerate *Dinophysis* cell-cycle stages, the concentrated water samples (2.5 L filtered and resuspended in 50 mL, concentration factor 1/50) were left to sediment over 12 h and the whole surface of the chamber scanned under the inverted microscope at ×100, so the detection level ranged from 0.8 to 2 cells $L^{-1}$.

*In situ* division rates were estimated, with a post-mitotic index approach, from the frequency of dividing (paired) and recently divided (incomplete development of the left sulcal list) cells, which were recognized by their distinct morphology as described in Reguera et al. (2003), following the model of Carpenter and Chang (1988):

$$\mu = \frac{1}{n(T_c + T_r)} \sum_{i=1}^{n} (t|s)_i ln[1 + f_c(t_i) + f_r(t_i)] \quad (2)$$

where $\mu$ is the daily average specific division rate, $f_c(t_i)$ is the frequency of cells in the cytokinetic (or paired cells) phase ($c$) and $f_r(t_i)$ is the half frequency of cells in the recently divided (incomplete development of the left sulcal list) ($r$) phase in the $i^{th}$ sample. $T_c$ and $T_r$ are the duration of the $c$ and $r$ phases, considered as "terminal events" (sensu Carpenter and Chang, 1988) in this work; $n$ is the number of samples taken in a 24-h cycle, and $t_s$ is the sampling interval in hours. The duration of the selected terminal events, $T_c + T_r$, was estimated as the interval of time necessary for a cohort of cells to pass from one phase to the next; in this case, the time interval between the time $t_0$—when the frequency of cells undergoing cytokinesis, $f_c$, is maximum—and the time $t_1$ when the fraction of recently divided cells $f_r$ is maximum:

$$\frac{1}{2}(T_c + T_r) = (t_0 - t_1) \quad (3)$$

where $T_c$, $T_r$, $t_1$ and $t_0$ are calculated after fitting a 5th degree Gaussian

function to the frequency data. Frequency of different cell-cycle stages was quantified only in samples providing a minimum number of specimens (n > 200) to have statistically sound results.

For comparative purposes, the vertical distribution of the lower bound of division rates ($\mu_{min}$) at peak-division time (06.00 GMT) was estimated from a single vertical profile at one shelf station (100 m deep) off Ría de Vigo on June 21. The 'maximum frequency approach' (McDuff and Chisholm, 1982) was used to estimate $\mu_{min}$ at each depth z, $(\mu_{min})_z$:

$$\mu_{min} = ln(1 + f_{max}) \quad (4)$$

where $f_{max}$ is the frequency of dividing cells at each depth. This approach assumes that all cells which divide in a given day can be recognized as undergoing or just completed mitosis, in one single sample collected at the time-window when maximal division is expected.

## 3. Results

### 3.1. Hydrographic conditions before and during the cruise

June 2013 showed a succession of short-term (5–14 days) upwelling-downwelling cycles which is a common feature during the upwelling season in the study area (Alvarez-Salgado et al, 2003). Nevertheless, daily average Ekman's transport estimate ($751 \pm 1201\ m^3\ s^{-1}\ km^{-1}$), with a maximal value of $2587\ m^3\ s^{-1}\ km^{-1}$ on June 23, showed a strong positive anomaly in relation to the historic mean (1985–2013) for June ($373 \pm 363\ m^3\ s^{-1}\ km^{-1}$) (Fig. 2A) (Díaz et al., 2016). Northerly winds with a mean velocity of $8.1\ m\ s^{-1}$ and a maximum of $10.5\ m\ s^{-1}$ on June 19 (Fig. 2B), were predominant during the cruise, which started with neap tides (Fig. 2C).

Hydrographic conditions in two longitudinal Ría de Vigo and Ría de Pontevedra-shelf transects showed common patterns in their response to a transition, that had occurred 2 days before (June 16), from relaxation to upwelling. These included shoaling of the isotherms (not so clear in Fig. 3A because of the missing stations in the outer reaches of Ría de Vigo) and a quick drop of temperature (> 2 °C) in the top 10 m of the two rías (Fig. 3). A higher resolution examination during the 36-h study showed that maximal gradients of temperature and salinity were found at 18–19 m at the beginning of the cruise (Fig. 4B–C), and at 10 m 26 h later. A prominent thin fluorescence layer was formed and followed the excursions of the pycnocline (Fig. 4D). Wind velocities, obtained from the meteorological station on board R/V *Ramón Margalef,* were very variable, with a mean velocity of $4.3\ m\ s^{-1}$. From 08:00 h to 20:00 h on June 19, a significant increase in northerly winds velocity was observed, with a maximum of $12.6\ m\ s^{-1}$ at 15:00 h (Fig. 4A). Nevertheless, from 20:00 h onwards there was a progressive decline, with values lower than $1\ m\ s^{-1}$ at the end of the 36-h cycle study. At the same time, high ($\sim 10^{-4}\ m^2\ s^{-3}$) near surface values of turbulence (ε), with maxima from 00:00 h to 02:00 h and 10:00 h to 14:00 h on June 19 and from 20:00 h (June 19) to 02:00 h on June 20, were observed, followed by a progressive decline the last day (June 20) from 04:00 h onwards. Values of ε at the depth of the thin layer, delimited by the 13.5–14 °C isotherms, increased from $10^{-8}\ m^2\ s^{-3}$ at the beginning of the cycle study (20:00 h on June 18) to $10^{-6}\ m^2\ s^{-3}$ (00:00 h on June 19). These changes coincided with the progressive shoaling of the thin layer that reached a 10 m depth between 00:00 h and 02:00 h on June 20. Thus, the uprising velocity of the inflowing water was around $0.34\ m\ h^{-1}$, and the thin layer was always associated with the pycnocline (Fig. 4F–I).

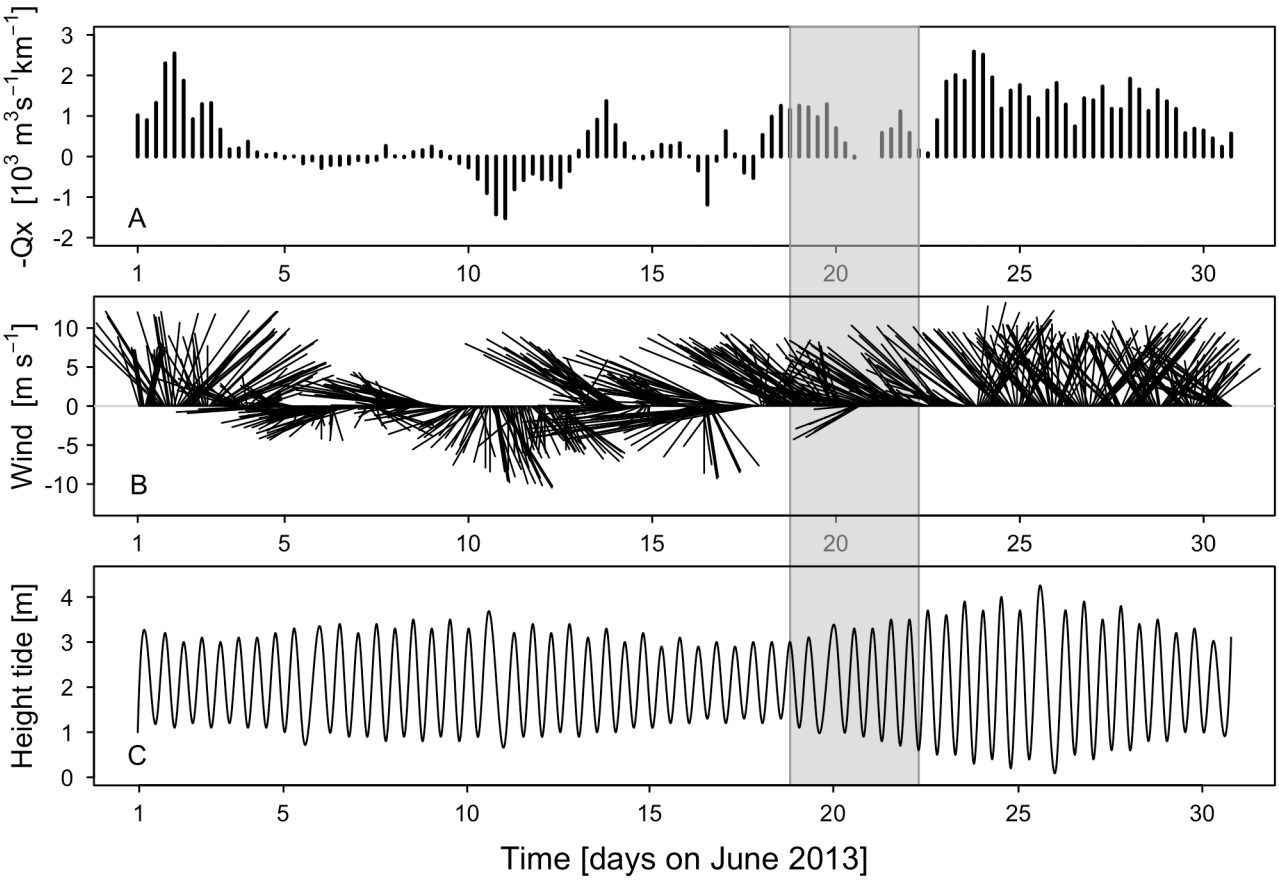


**Fig 2.** Time series of (A) Estimates of daily upwelling indices, $Q_x$ ($m^3\ s^{-1}\ km^{-1}$) (positive values indicate upwelling), estimated from Silleiro buoy (Western Galicia) data, during June 2013, (B) vector diagram of wind direction and velocity ($m\ s^{-1}$) recorded hourly at the Cabo Silleiro buoy (positive values correspond to northerly winds) and C) sea level (m) recorded hourly. Shaded area indicates the days of the cruise.

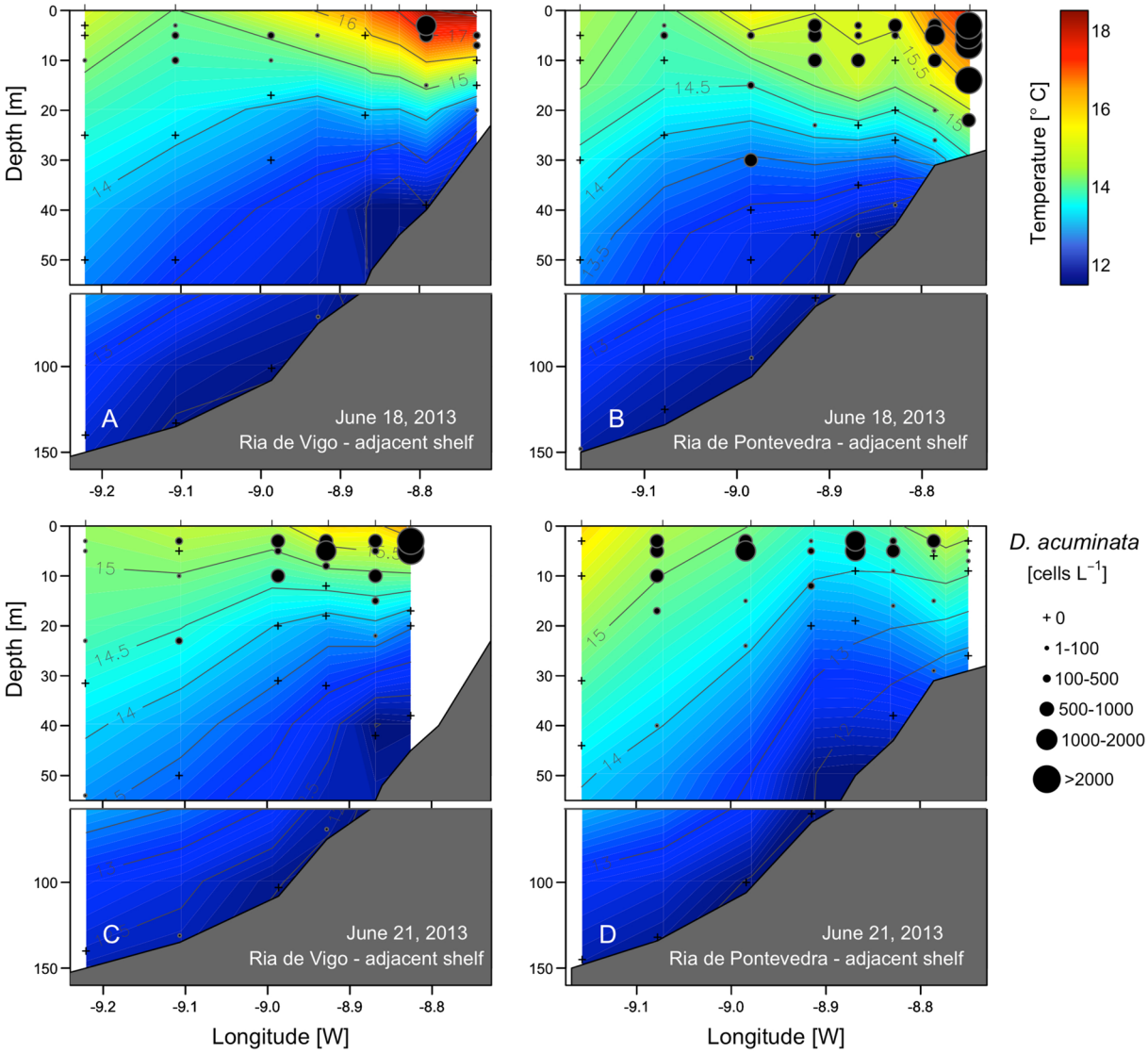


**Fig. 3.** Vertical distribution of temperature (°C) and *D. acuminata* (cells $L^{-1}$) in ría-shelf transects from Ría de Vigo (A, C) and Ría de Pontevedra (B, D) on June 18 and June 21.

Currents from the ADCP moored at the centre of the navigation channel (red square in Fig. 1, close to the position of the 36 h study) showed the currents variability in response to tides and to the northerly (upwelling) and southerly (downwelling) winds (Fig. 5). Before the cruise, a downwelling event on June 16 was associated with surface inflow and also with northward cross-channel flow (Fig. 5A, B). Tidal modulation of the currents was observed although the downwelling event occurred near neap tides. After this downwelling event, weak upwelling was associated on June 18 midday with inflow in the bottom layers and a near surface outflow, modulated by tides, of the water previously retained in the inner parts of the ria during downwelling. The outflowing layer became progressively thinner while the inflow layer increased (Fig. 5A). The tidal signal was clearer when the cycle study began (June 18 night). During the rest of the cycle, inflow and outflow occurred during ebb and flood (tidal amplitude was increasing), although upwelling conditions until relaxation on June 20 modulated the currents due to the upwelling-induced surface outflow and bottom inflow. After the cycle, the tidal signal was clear too, and again modulated by the peak of the upwelling-induced surface outflow on June 22.

Results of model simulations for sea surface temperature (SST) and current velocities confirmed changes from weak inflowing currents favouring retention inside the rías on June 16 to strong outflowing currents from June 18 (the day of initiation of the 36-h study) onwards (Fig. 6). From June 19, these simulations revealed the presence of cold (~14 °C) upwelled surface water along the Galician coast, to the south of Ría de Vigo. Although the model did not resolve in detail the circulation inside the Ria due to the coarse resolution (1 km), it was possible to assess variability of the inflow-outflow into the Ría, and a picture compatible with that depicted by the ADCP was obtained.

### 3.2. Distribution of Dinophysis and other dinoflagellate species and ciliates

During relaxation, longitudinal ría-shelf transects showed that maximal densities of *Dinophysis* ($1 \times 10^3$ cells $L^{-1}$) near the surface (3–5 m) in the inner reaches of the rías were located in the warm (> 16 °C) water layer, most likely advected from the shelf the previous days (Fig. 3A–B). After the upwelling pulse, mixed surface waters cooled down (< 15 °C) and *Dinophysis* maxima ($2.2 \times 10^3$ cells $L^{-1}$), located in the top 5 m of the water column, moved off to the outer reaches of the rías and shelf waters (Fig. 3C–D).

Data from the Galician Monitoring Centre on the distribution of *Dinophysis* (integrated tube-samples) in Ría de Pontevedra (10 stations) the weeks before, during and after the cruise (Fig. 7) support the idea of

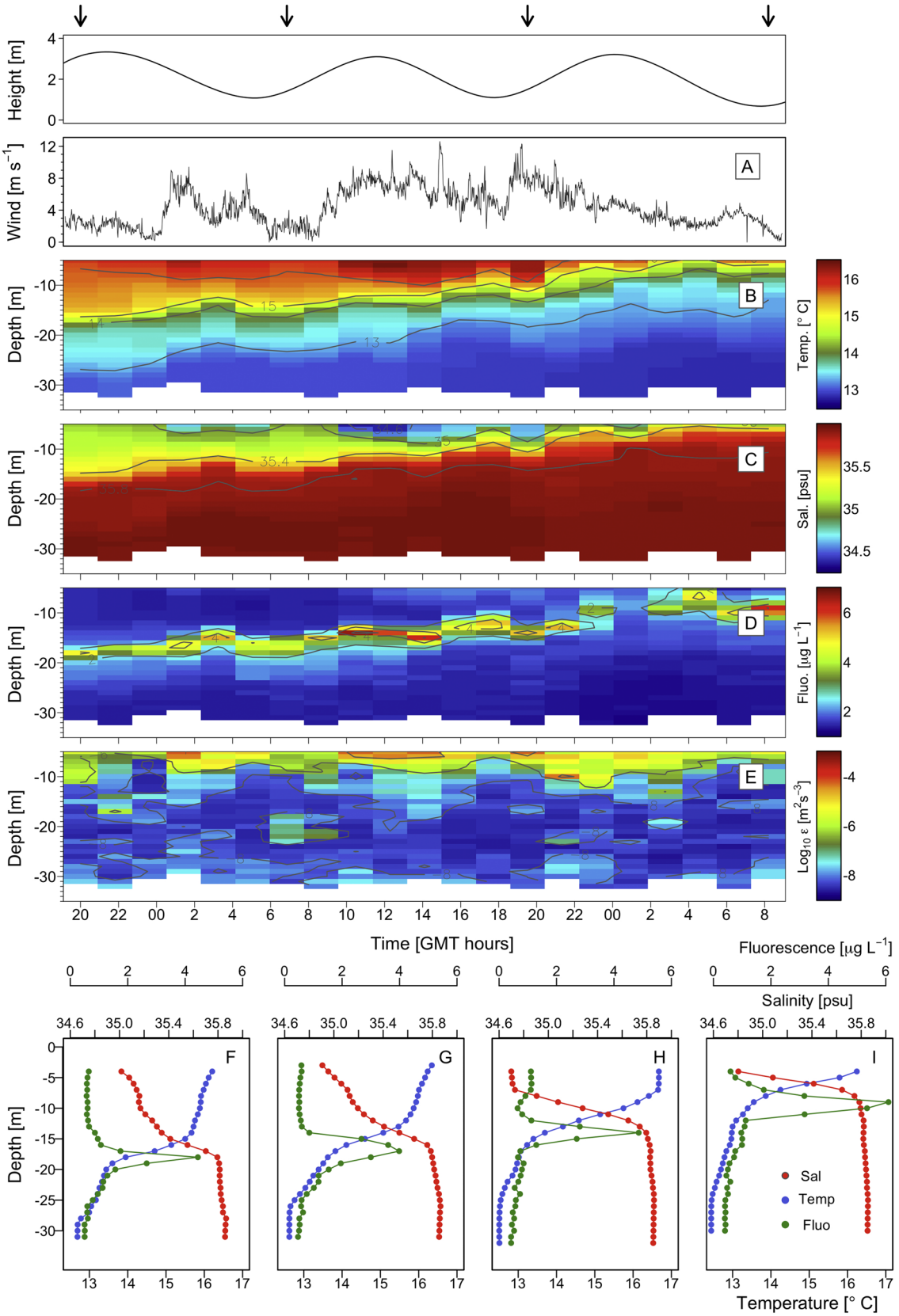


**Fig. 4.** Vertical distribution of (A) Wind velocities recorded every 1-minute on board R/V *Ramón Margalef*; (B) Temperature; (C) Salinity, (D) *In vivo* fluorescence and E) Turbulent kinetic energy dissipation rate ($\varepsilon$) derived from the microstructure profiler deployed at a fixed station (P2) during the 36-h cycle study, 18–20 June 2013. Arrows in the top panel (sea level) indicate the hours corresponding to the vertical profiles of the temperature, salinity and fluorescence shown below (F-E).

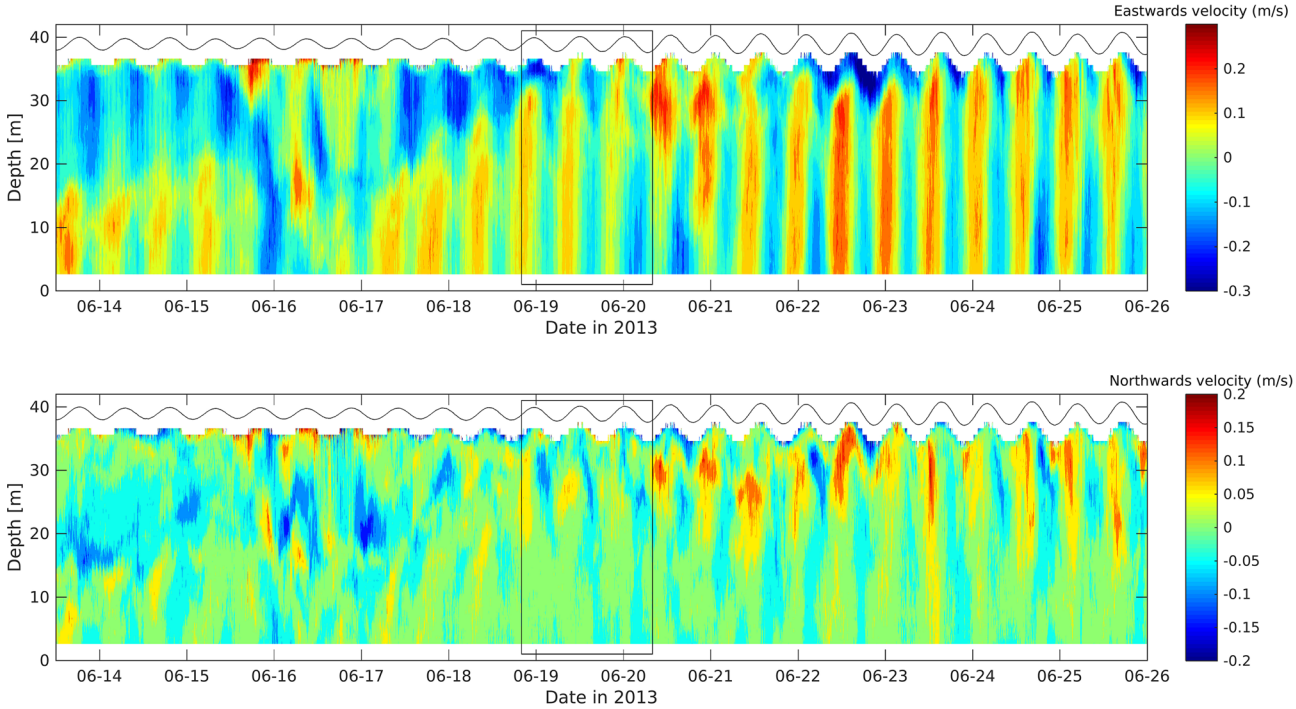


**Fig. 5.** Eastwards (top panel) and northwards (bottom panel) current velocity components (instantaneous flow variability) from the bottom mounted ADCP at station P3 in Ría de Pontevedra between 14 and 26 June. ADCP pressure sensor is plotted as a reference.

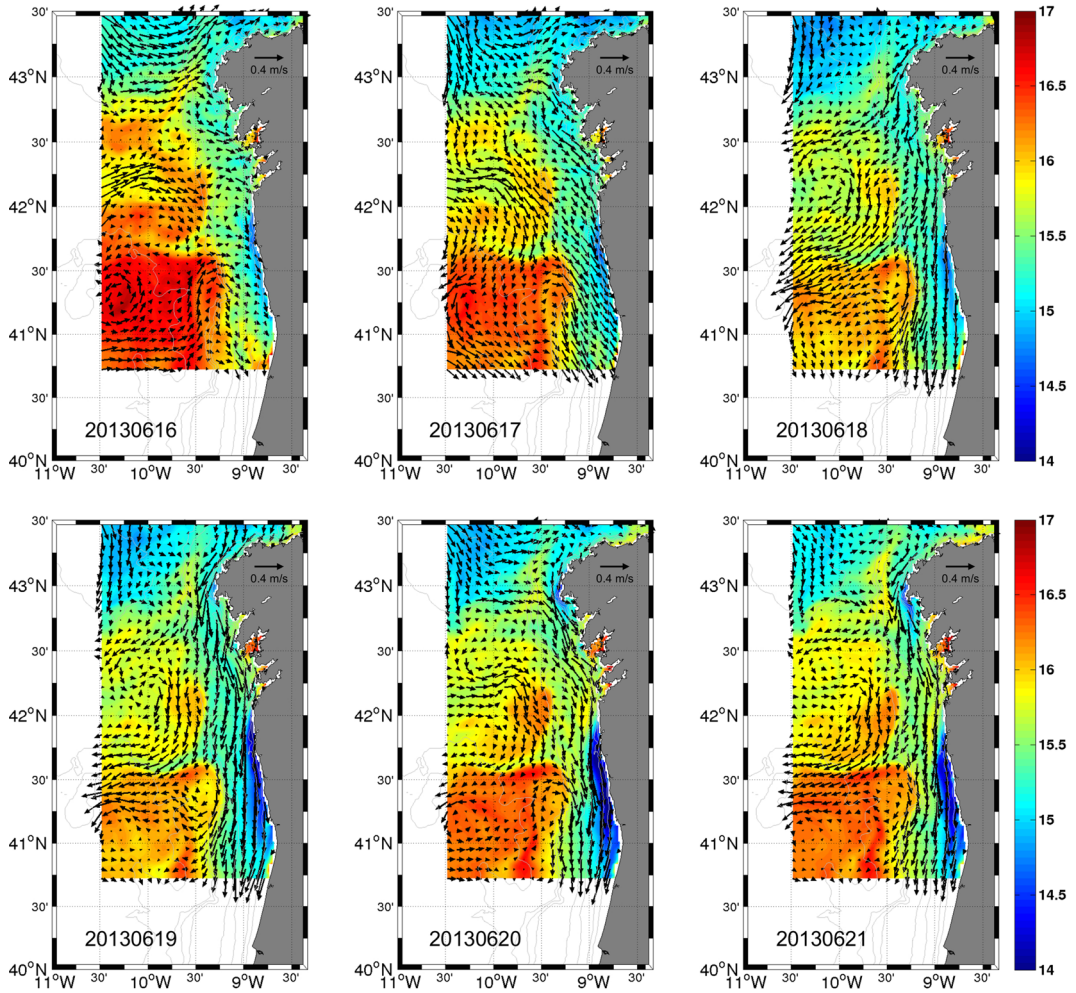


**Fig. 6.** Model generated distribution of daily sea surface temperature (SST) (°C) and surface currents from June 16 to 21.

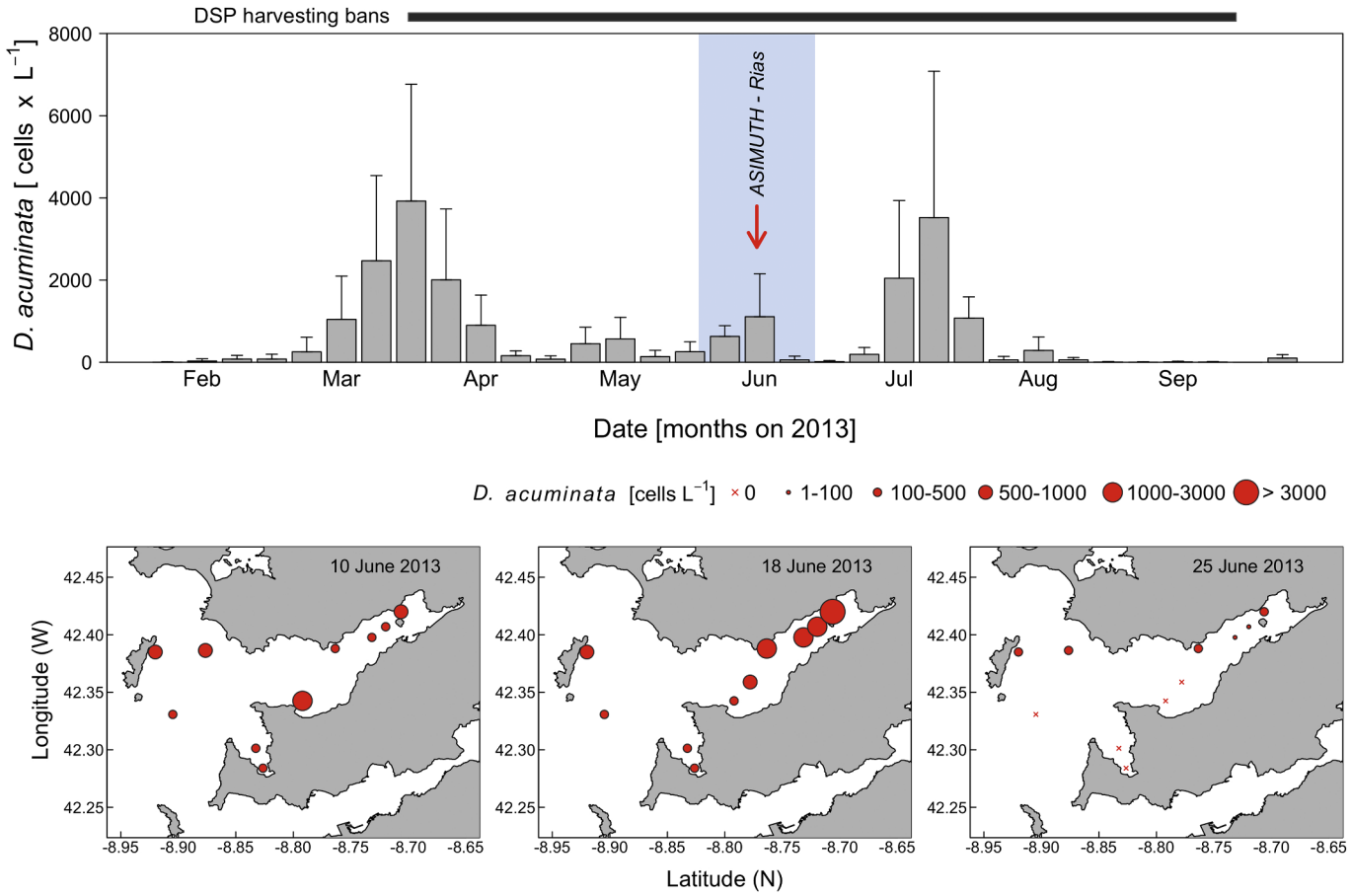


**Fig. 7.** Weekly variation of *Dinophysis acuminata* cell densities (data from the Galician Monitoring Centre) in Ría de Pontevedra (mean of 10 monitoring stations) from February to September 2013 (top panel) and spatial distribution of *D. acuminata* cell maxima in Ría de Pontevedra before (June 10), during (June 18) and after (June 25) the cruise *ASIMUTH-Rías* 2013. Error bars in the top panel represent mean and standard deviation (n = 10).

advection into and out of the ría suggested before (Fig. 5). Prior to the cruise (June 10), *D. acuminata* cell densities ranged between 280 and 1240 cells $L^{-1}$. The week of the cruise (June 18), relaxation-driven cross-shelf transport led to a *Dinophysis* cell maximum ($> 3 \times 10^3$ cells $L^{-1}$) in the innermost part of the ría. The ADCP records provided evidence of this transport between 15 and 17 of June (Fig. 5). The surface outflow during ebb tide coincided with the observation of a dense population of *Dinophysis* on June 18. The population decline observed during the cycle was depicted in the following week's monitoring results (June 25) from Ría de Pontevedra (Fig. 7).

During the 36-h cycle study, vertical haul-samples from the top 15 m showed the low-density microplankton community was dominated by large chain-forming diatoms (*Detonula pumila*, *Thalassiosira rotula*, *Chaetoceros spp*) with half-empty cells and a decaying appearance in addition to detritus. The most striking temporal change was the sudden inflow of *Protoperidinium* spp. (*P. conicum*, *P. divergens*, *P. diabolum*) between 12:00 h and 20:00 h on June 19 (Table 1). Remarkable changes were also observed in *D. acuminata*, the most abundant dinoflagellate species throughout the study. Densities in the vertical net hauls ranged from 7 to 8 cells $mL^{-1}$ at 20:00 h on June 18 to 150–170 cells $mL^{-1}$ at 16:00–18:00 h on June 19. These extreme values coincided with high and low tide respectively (Table 1).

From all the analysed samples collected at discrete depths, there was no evidence of daily vertical migration of *D. acuminata* during the 36 h study, and cell maxima remained in the warmer (> 16 °C) and more brackish (< 35) surface layer, above the 25.4 $\sigma_t$ isopycnal (Fig. 8A). Cell densities increased during the outward tidal flow (ebb tide), and the cell maximum, $2.4 \times 10^3$ cell $L^{-1}$, at 5 m, was observed at 03.00 on June 19, coinciding—as in the haul samples—with low tide.

In contrast *Mesodinium* cells with marked morphological variability, probably including at least two species (*Mesodinium rubrum* and *M. major*), showed maximal cell densities below the pycnocline at night, but aggregated at the surface between 14:00 h and 16:00 h, the only time window when they overlapped the *Dinophysis* cell maxima (Fig. 8A). As in the case of *Dinophysis*, the ciliate cell maximum ($5 \times 10^3$ cell $L^{-1}$), was observed at the surface (3 m), on June 19 at low tide. *Mesodinium* spp. were the main component of the microzooplanktonic ciliate populations at peak hours (14:00 to 16:00 h in the afternoon and 02:00–04:00 h at night (Fig. 8B). Other identified plastid-retaining ciliate species, such as *Laboea strobila, Strombidium spiralis, Strombidium acutum* and *Strombidium epidemum* reached high densities, sometimes overtaking *Mesodinium's* dominance. In addition, a relevant contribution of ciliates for which retained plastids have not been described, including *Legaardiella sol*, *L. ovalis*, *Lomhaniella oviformis* and the well known prey of the heterotrophic *Phalacroma rotundatum*, *Tiarina fusus* (Fig. 8B) was noted. Attention should be paid to a second cell maximum of *Dinophysis* near the bottom which appeared on three occasions just before low tide (Fig. 8A).

### 3.3. Estimates of μ and particulate and dissolved toxins during the 36 h study

Monitoring for 36 h at the fixed station the fraction of cells undergoing mitosis showed that there were marked differences in frequencies of mitotic cells at different depths (Table 2). Maximal frequencies were observed at 3–7 m—above the 25.4 $\sigma_t$ isopycnal—where the cell maxima were found throughout the two cycles on June 19 and June 20. Frequencies observed in the cell-maximum layer were used to estimate

**Table 1**
Cell densities of dinoflagellate species in 20 µm vertical net-hauls (relative abundance), collected for toxin analyses during the 36-h cycle from June 18 to June 20, 2013.

| | Sampling hour (GMT) | | | | | | | | | | | | | | | | | | |
|---|---|---|---|---|---|---|---|---|---|---|---|---|---|---|---|---|---|---|---|
| | 20 | 22 | 0 | 2 | 4 | 6 | 8 | 10 | 12 | 14 | 16 | 18 | 20 | 22 | 0 | 2 | 4 | 6 | 8 |
| *Dinophysis acuminata* | 8 | 7 | 53 | 183 | 76 | 74 | 115 | 76 | 137 | 62 | 170 | 153 | 36 | 50 | 23 | 21 | 27 | 19 | 23 |
| *Dinophysis acuta* | 0 | 0 | 0 | 0 | 0 | 0 | 0 | 0 | 0 | 0 | 0 | 0.3 | 0 | 0 | 0 | 0 | 0 | 0 | 0 |
| *Phalachroma rotundatum* | 0.3 | 0 | 0.3 | 1 | 0.3 | 3 | 2 | 1 | 0 | 1 | 2 | 1 | 2 | 2 | 1 | 1 | 0 | 2 | 1 |
| *Protoperidinium* sp. | | | | | | | | | | | | | | | | | | | |
| *P. claudicans* | 0 | 0 | 0 | 0 | 0 | 0.3 | 1 | 1 | 1 | 0 | 2 | 0 | 0 | 0 | 0 | 0.3 | 1 | 0 | 0 |
| *P. cerasus* | 0 | 0 | 0 | 0 | 0 | 0 | 0 | 0 | 0 | 0 | 0.3 | 0 | 0 | 0 | 0 | 0 | 0 | 0 | 0 |
| *P.* cf *conicum* | 1 | 1 | 2 | 2 | 1 | 1 | 2 | 1 | 18 | 6 | 36 | 28 | 8 | 10 | 8 | 11 | 7 | 6 | 33 |
| *P.* cf *divergens* | 1 | 0.3 | 8 | 2 | 2 | 4 | 11 | 3 | 10 | 4 | 22 | 30 | 7 | 5 | 3 | 3 | 2 | 3 | 5 |
| *P. depressum* | 0.3 | 0 | 1 | 0 | 0 | 0.3 | 0.3 | 1 | 0 | 0 | 0.3 | 0 | 0 | 0 | 0 | 0 | 1 | 0 | 0 |
| *P. diabolus* | 5 | 1 | 8 | 7 | 4 | 12 | 25 | 4 | 105 | 23 | 78 | 77 | 19 | 9 | 5 | 12 | 9 | 10 | 14 |
| *P. mite* | 0.3 | 1 | 1 | 0.3 | 1 | 1 | 1 | 1 | 1 | 1 | 0 | 0.3 | 0.3 | 0 | 0.3 | 1 | 0.3 | 0 | 0.3 |
| *P. oblongum* | 0 | 0 | 0 | 0 | 0 | 0 | 0 | 0 | 0 | 0 | 0 | 1 | 0.3 | 0 | 0 | 0 | 0 | 1 | 2 |
| *P. oceanicum* | 0 | 0 | 0 | 0.3 | 0 | 0 | 0 | 0 | 0 | 0 | 0.3 | 0 | 0 | 0 | 0 | 0 | 0 | 0 | 0 |
| *P. ovatum* + *Diplopsalis* | 3 | 0 | 0 | 0 | 0 | 0 | 0 | 0 | 0 | 0 | 0 | 0 | 0 | 0 | 0 | 0 | 0 | 0 | 0 |
| *Protoperidinium* spp. | 0 | 0 | 0 | 0.3 | 0 | 0.3 | 0.3 | 0 | 0 | 0 | 0 | 0 | 0 | 1 | 1 | 1 | 0 | 0 | 0 |
| *Other dinoflagellates* | | | | | | | | | | | | | | | | | | | |
| *Tripos falcatum* | 0 | 0 | 0 | 0 | 0 | 0 | 0 | 0 | 0.3 | 0 | 0 | 0 | 0 | 0 | 0 | 0 | 0 | 0 | 0 |
| *Tripos furca* | 3 | 0.3 | 7 | 8 | 1 | 0 | 2 | 6 | 3 | 2 | 4 | 3 | 1 | 1 | 3 | 1 | 2 | 0.3 | 2 |
| *Tripos fusus* | 2 | 0.3 | 1 | 2 | 0 | 1 | 0.3 | 5 | 1 | 0 | 0 | 0.3 | 0 | 0 | 0.3 | 1 | 0 | 0.3 | 0 |
| *Tripos macroceros* | 0 | 0 | 0 | 0 | 0 | 0 | 0 | 1 | 0 | 0 | 0 | 0 | 0 | 0 | 0 | 0 | 0 | 0 | 0 |
| *Tripos setaceum* | 0 | 0 | 0 | 0.3 | 0 | 0 | 0 | 0 | 0 | 0.3 | 0.3 | 0.3 | 0 | 0 | 0 | 0 | 0 | 0 | 0.3 |
| *Diplopsalis lenticula* | 0 | 2 | 8 | 12 | 5 | 7 | 7 | 4 | 24 | 6 | 22 | 19 | 6 | 3 | 3 | 5 | 2 | 6 | 11 |
| *Gonyaulax* sp. | 0 | 0 | 0 | 0 | 0 | 0 | 0 | 0 | 0 | 0 | 1 | 0 | 0 | 0 | 0 | 0 | 0 | 0 | 0 |
| *Gymnodinium* sp. | 0 | 0 | 0 | 0 | 0 | 0 | 0 | 0 | 0.3 | 0 | 0 | 0 | 0 | 0 | 0 | 0 | 0 | 0 | 0 |
| *Gyrodinium lachrima* | 0 | 0 | 0 | 0 | 0 | 0 | 0 | 0 | 0 | 0 | 0 | 0 | 0 | 0.3 | 0 | 0 | 0 | 0 | 0 |
| *Gyrodinium* spp. | 0 | 0 | 0 | 0.3 | 0 | 0 | 0 | 0 | 0 | 0 | 0 | 0 | 0 | 0 | 0 | 1 | 0 | 0 | 0.3 |
| Peridinioide | 0 | 0 | 0 | 0 | 0 | 0 | 0 | 0 | 0 | 0 | 1 | 0 | 0 | 0 | 0 | 0 | 0 | 0 | 0 |
| *Prorocentrum micans* | 1 | 1 | 8 | 9 | 2 | 2 | 3 | 1 | 9 | 2 | 16 | 22 | 6 | 5 | 2 | 2 | 2 | 2 | 3 |
| *Pyrocystis lunula* | 0.3 | 0 | 1 | 1 | 1 | 1 | 2 | 1 | 0 | 0 | 4 | 3 | 1 | 3 | 1 | 3 | 0 | 0 | 2 |
| Total | 25 | 14 | 98 | 229 | 93 | 107 | 172 | 104 | 312 | 107 | 359 | 338 | 88 | 90 | 51 | 62 | 53 | 48 | 97 |

$\mu_{avg}$ according to Carpenter's model (Carpenter and Chang, 1988). Cell densities below 5–7 m were too low in most cases to make statistically significant estimates of division rates.

Distribution of frequencies of dividing ($f_c$) and recently divided ($f_r$) cells of *D. acuminata* showed a clear-cut phased cell division on June 19 and June 20, but maximal frequency of dividing cells ($f_c + f_r$) on June 19, 0.48, was almost threefold the value estimated for June 20 (0.18) (Fig. 9A). Slight differences were also found in the timing of the maximal frequencies of dividing plus recently divided cells (06:00 h and 05:00 h GMT), i.e. maximum $f_c$ was just at dawn (06:00 h) on June 19 and one hour earlier on June 20. Thus, estimates of $\mu_{avg}$ and $\mu_{min}$ were 0.65 $d^{-1}$ and 0.39 $d^{-1}$ on June 19 and 0.33 $d^{-1}$ and 0.17 $d^{-1}$ on June 20, respectively. Nevertheless, the time lag between the peaks of cytokinesis and sulcal-list regeneration was the same (1 h) on both days, although the distribution of recently divided cells ($f_r$) showed a sharper curve the first days.

Estimates of toxin (OA) content per cell, i.e. toxin accumulation, showed a maximum (11.4 pg OA $cell^{-1}$) at 06.00 h on June 19 and a second maximum (8.7 pg OA $cell^{-1}$) at 22.00 h on June 20 (Fig. 9B). The largest difference was observed between 06:00 h and 08.00 h on June 19. Toxin concentrations in the net-haul filtrate ("dissolved toxins"), with three maxima observed at 02:00 h, 12:00 h and 16:00 h on June 19 (0.75, 0.59, 0.27 pg OA $mL^{-1}$ respectively) were negligible, and below detection limits on June 20 (Fig. 9B).

### 3.4. Vertical profiles and distribution of $\mu_{min}$ on the shelf stations

Vertical distributions of physical properties at two shelf stations (V5 and V6; ~100 m deep) off Ría de Vigo on June 18 and 21 (Figs. 10, 11) showed that changes in water column structure there were not as pronounced as inside the rías, although the pycnocline (from 18 to 35 m) observed at station V6 on June 18 (Fig. 11A) had been eroded. Likewise, changes in the vertical distribution of turbulent kinetic energy dissipation rates ($\varepsilon$) above the pycnocline were not relevant at V5, the shelf station, before and after the cycle study (Fig. 10A, C), although $\varepsilon$ increased between 30 and 50 m and in the bottom layer on June 21. Nevertheless, at both stations and both before and after the 36-h cycle, maximal densities of *D. acuminata* (1200 cells $L^{-1}$) were observed at 5 m (Figs. 10B, D; 11C).

Vertical distribution of *Mesodinium*, restricted to the top 15 m, coincided with the vertical range of *D. acuminata*. Maxima (> 1000 cells $L^{-1}$) of the two species co-occurred at 08.00 h, at 5 m on June 21 (Fig. 10D) at station V5. Likewise, the *Dinophysis* cell maximum was at 5 m, and coincided with the diatom and dinoflagellate cell maxima at the outer shelf station V6, at 06.00 h GMT on June 21 (Fig. 11D). The very low density diatom maximum (~5000 cells $L^{-1}$) was dominated by *Proboscia alata* (46%) and *Pseudo-nitzschia* cf *seriata* (25%), and the dinoflagellate maximum by *D. acuminata* (90%). Distribution of $\mu_{min}$ (the lower bound of division rate) at each depth $(\mu_{min})_z$ during peak-division time (06.00 h GMT, i.e., the sampling time) on June 21 showed that a very high value of $\mu_{min}$ (0.69 $d^{-1}$) was not found in the layer of the cell maximum (5 m) but between 11 and 17 m, where cell densities were much lower (Fig. 11C). Still the value of $\mu_{min}$ (0.36 $d^{-1}$) at the cell maximum was identical to that estimated inside the rías from June 18 to 19 and before the intrusion of cold water. In contrast, $\mu_{min}$ values at the cell maxima inside the ría dropped from 0.39 to 0.17 $d^{-1}$ by the end of the cycle study (June 20).

## 4. Discussion

The survey for the present study took place during a relaxation–upwelling transition in the Galician Rías Baixas which had been

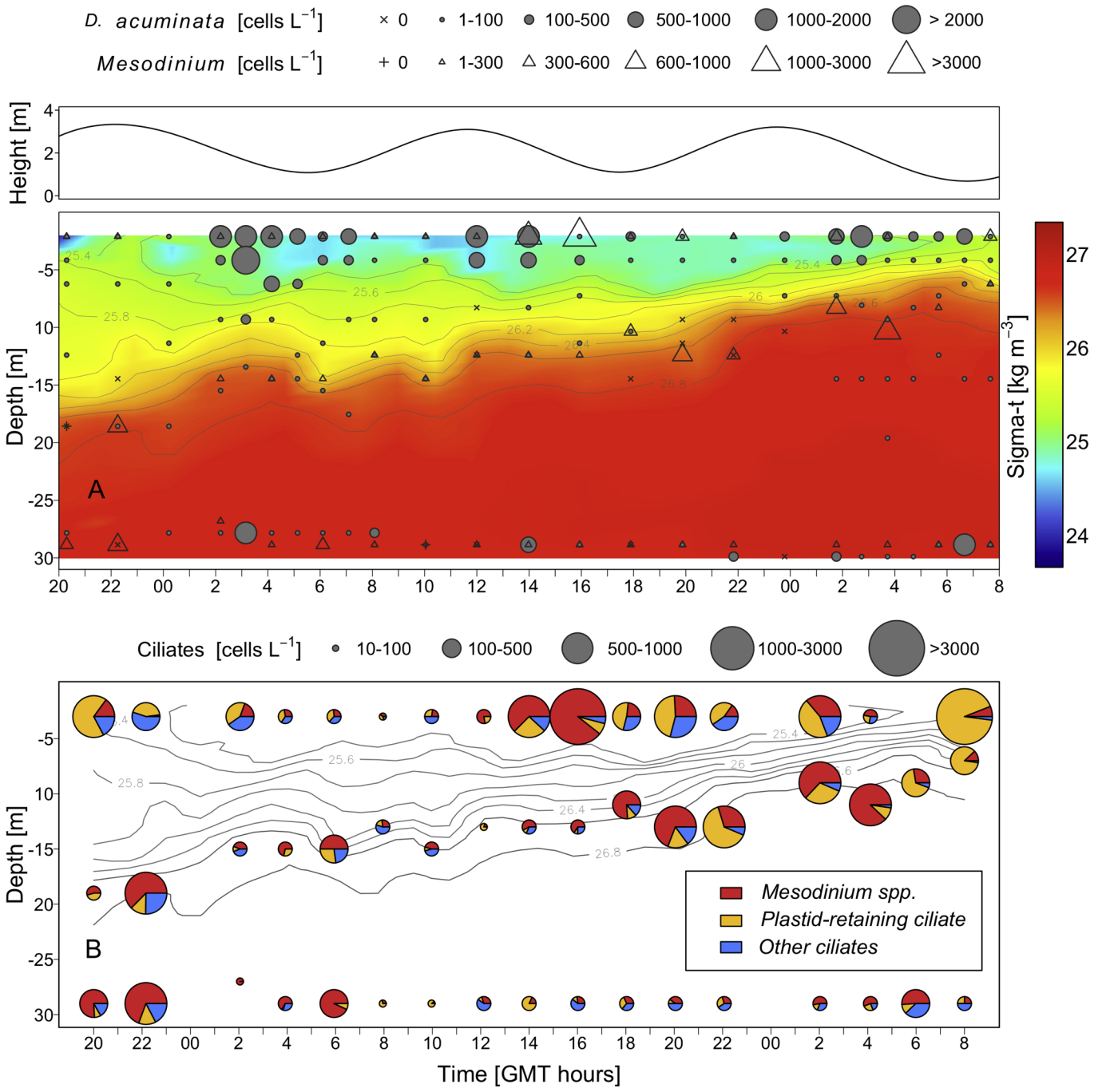


**Fig. 8.** Vertical distribution of (A) seawater density, *Dinophysis acuminata* (cells $L^{-1}$) and *Mesodinium* cells (cells $L^{-1}$); (B) total number of microplanktonic ciliates (cells $L^{-1}$) separate in three classes (*Mesodimium* spp., plastid-retaining ciliate and others ciliate) at a fixed station (P2) during a 36-h cell-cycle study, 18–20 June 2013. Sea level (m), recorded hourly, is indicated in the top panel.

preceded by a downwelling event. Changes in thermohaline structure showed a rapid response to the wind-induced upwelling pulse. The onset of upwelling the second day of the cruise was characterized by the well known ascent of nutrient-rich ENAC water towards the coast and shoaling of an already established thin layer of diatoms, dominated by *Pseudo-nitzschia* spp. and *Proboscia alata*. In addition, the distribution of the DSP toxin producer *D. acuminata* and accompanying microplanktonic ciliates, and the impact of the abrupt changes of the water column structure on the physiological status of *Dinophysis* were explored.

### 4.1. Coupling of physical-biological processes

Earlier studies in the Galician Rías Baixas using high resolution sampling instruments showed the coupling between maximum values of shear and buoyancy frequency as the mechanism behind the shaping of a subsurface chlorophyll maximum (SCM) into a thin layer under upwelling conditions (Velo-Suárez et al., 2010). Later studies showed the role of tidal (both semidiurnal and spring–neap) variability as a modulator of the response of the Ría circulation to wind-induced upwelling (Díaz et al., 2014). Here, the additional use of a turbulence profiler

**Table 2**
Vertical distribution of *Dinophysis acuminata* cells (total number of specimen observed in 2.5 L), scanned to estimate the frequency of cells undergoing mitosis (n% in brackets) at a monitored fixed station (P2) during a 36-h study from 18 to 20 June 2013.

| Depths | Sampling hour (GMT) | | | | | | | | | | | |
|---|---|---|---|---|---|---|---|---|---|---|---|---|
| | 20 | 22 | 0 | 2 | 3 | 4 | 5 | 6 | 7 | 8 | 10 | 12 |
| 3 | 19 (0) | 64 (0) | 248 (0) | 3462 (2.2) | 4045 (7.3) | 4052 (18.7) | 2038 (30.7) | 415 (32.3) | 2379 (14.5) | 80 (7.0) | 184 (0.7) | 3656 (0) |
| 5 | 7 (0) | | | 1173 (1.9) | 6112 (4.1) | | | 669 (25.4) | 681 (13.4) | 43 (7.0) | 52 (0.7) | 1517 (0) |
| 7 | 24 (0) | 12 (0) | 32 (0) | | | 1892 (16.6) | 397 (29.2) | | | | | |
| 8 | | | | | | | | | | | | |
| 9 | | | | | | | | | | | | 1 (0) |
| 10 | | | | 10 (0) | 292 (5.1) | 47 (6.4) | | | 2 (0) | 4 (0) | 4 (0) | |
| 11 | | | | | | | | | | | | |
| 12 | | | 5 (0) | | | | | 50 (32.0) | | | | |
| 13 | 3 (0) | | | | | | 27 (0) | | | 17 (0) | | 1 (0) |
| 14 | | | | | 220 (1.8) | | | | | | | |
| 15 | | 1 (0) | | | | 45 (2.2) | 25 (0) | | | | 5 (0) | |
| 16 | | | | 14 (0) | | | | 56 (19.6) | | | | |
| 18 | | | | | | | | | 2 (0) | | | |
| 19 | 1 (0) | 4 (0) | 4 (0) | | | | | | | | | |
| 20 | | | | | | | | | | | | |
| 28 | 4 (0) | | 5 (0) | 22 (0) | 2819 (3.1) | 4 (0) | 21 (0) | 56 (17.9) | 56 (0) | 666 (14.4) | | |

(*continued on next page*)

**Table 2** (*continued*)

| Depths | Sampling hour (GMT) | | | | | | | | | | | |
|---|---|---|---|---|---|---|---|---|---|---|---|---|
| | 20 | 22 | 0 | 2 | 3 | 4 | 5 | 6 | 7 | 8 | 10 | 12 |
| 29 | | 1 (0) | | | | | | | | | 5 (0) | 0 (0) |
| 30 | | | | | | | | | | | | |

| Depths | Sampling hour (GMT) | | | | | | | | | | | | |
|---|---|---|---|---|---|---|---|---|---|---|---|---|---|
| | 14 | 16 | 18 | 20 | 22 | 0 | 2 | 3 | 4 | 5 | 6 | 7 | 8 |
| 3 | 3867 (0) | 205 (0) | 369 (0) | 214 (0) | 122 (0) | 331 (0.3) | 1690 (1.1) | 2678 (2.5) | 758 (10.2) | 871 (15.4) | 317 (12.6) | 1501 (7.5) | 68 (4.4) |
| 5 | 1513 (0.1) | 580 (0) | 210 (0) | 54 (0) | 23 (0) | 162 (0) | 543 (1.3) | 421 (1.7) | 231 (10.8) | 127 (11.8) | 15 (6.7) | 53 (9.4) | 45 (0) |
| 7 | | | | | | | | | | | | 19 (5.3) | 4 (0) |
| 8 | | 9 (0) | | | | 2 (0) | 27 (0) | | | | 18 (0) | | |
| 9 | 46 (0) | | | | | | | 82 (1.2) | | 12 (0) | | | |
| 10 | | | | 0 (0) | 1 (0) | | | | 3 (0) | | | | |
| 11 | | | 13 (0) | | | 0 (0) | | | | | | | |
| 12 | | 7 (0) | | 0 (0) | | | | | | | | | |
| 13 | 16 (0) | | | | 0 (0) | | | | | | 14 (0) | | |
| 14 | | | | | | | | | | | | | |
| 15 | | | 1 (0) | | | | 26 (0) | 13 (0) | 15 (0) | 14 (7.1) | | 39 (5.1) | 7 (0) |
| 16 | | | | | | | | | | | | | |
| 18 | | | | | | | | | | | | | |
| 19 | | | | | | | | | | | | | |
| 20 | | | | | | | | | 29 (3.4) | | | | |
| 28 | | | | | | | | | | | | | |
| 29 | 1311 (0.9) | 8 (0) | 0 (0) | 10 (0) | | | | | | | 35 (0) | 3377 (7.7) | 15 (0) |
| 30 | | | | | 545 (4) | 1 (0) | 643 (1.7) | 41 (4.9) | 22 (0) | 34 (0) | | | |

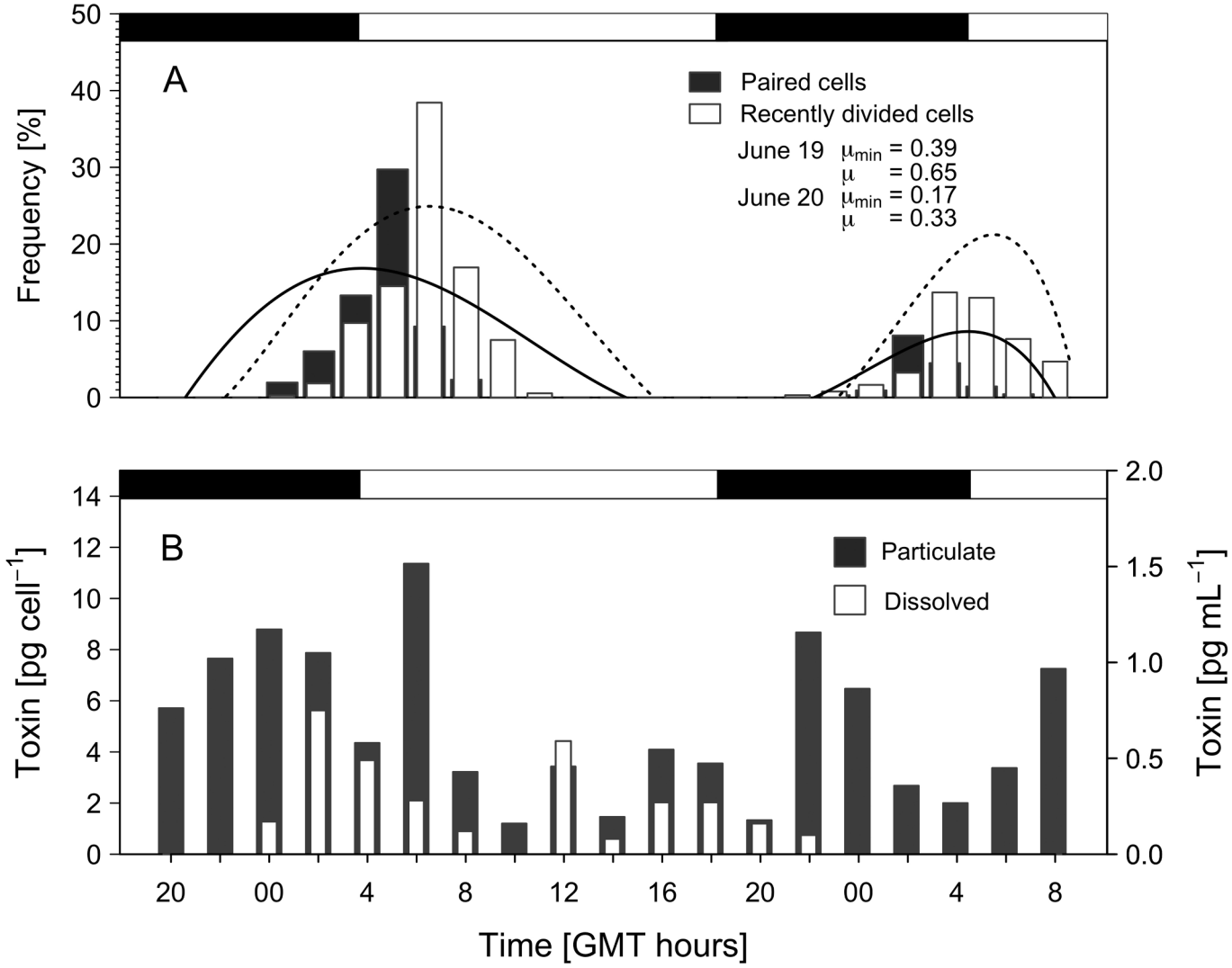


**Fig. 9.** Cell cycle study, 18–20 June 2013: (A) Distribution of frequencies of paired (dividing, black bars) and recently divided (white bars) cells of *D. acuminata*, fitted to a 5th degree polynomial curve; (B) Distribution of particulate toxin quota (pg OA cell$^{-1}$) (black bars) and dissolved toxins (ng mL$^{-1}$) (white bars). Black shading in top bar indicates period between sunset and sunrise.

allowed us to quantify the increased turbulence (ε) in the mixed layer, and to quantify the erosion of the shoaling thin layer of diatoms when it was exposed to turbulence levels of $10^{-5}$–$10^{-4}$ m$^2$ s$^{-3}$. This eroded thin layer, which formed again when turbulence dropped, rose from 18 m to 10 m during the cycle study, and appeared all the time constrained within the 13.5° and 14 °C isotherms and turbulence levels between $10^{-8}$ and $10^{-6}$ m$^2$ s$^{-3}$. Thus, the thin layer followed the excursions of the pycnocline, indicating a tight coupling between the chlorophyll maximum (dominated by diatoms) and the vertical gradients of water column density and turbulence, i.e. between the physical and biological processes.

In his pioneering work, Lasker (1978) described the interactions between wind strength and the aggregation of the dinoflagellate *Gymnodinium splendens (=Akashiwo sanguinea)* in high density (thin layers, undescribed in those days) layers as a requisite for a good first-feeding of anchovy larvae in Southern California waters. To form these layers, the *Akashiwo* population needed a period of at least four calm days with wind strength below 5 m s$^{-1}$. This wind-velocity threshold was well exceeded during our cycle study on June 19, when records from the research vessel meteorological station showed northerly wind velocities higher than 12 m s$^{-1}$ (Fig. 4A). Intensification of northerly winds, which had started on June 18, was associated with the increased turbulence, and coincided with a transient erosion of the thin layer as it rose to 10 m depth at 02:00 h on June 20.

### 4.2. Distribution of *D. acuminata* in relation to its prey during the relaxation-upwelling transition

Declining densities of *D. acuminata* during the flood tide (Fig. 8) support the view that the bulk of *Dinophysis* cells came from the innermost parts of the Ría where they had accumulated during relaxation. This adds to the picture of a net outward flow of *Dinophysis* cells from the ría to the adjacent shelf. The occurrence of a second *Dinophysis* maximum near the bottom at 03.00 AM on June 19, shortly before low tide (Fig. 8) is difficult to interpret. Cells in this bottom maximum, and those in a co-occurring surface maximum, had similar division frequencies (Table 2), so they were not likely to be sedimenting from the surface populations. One possibility is that these cells were injected into the ría with the upwelling waters, a mechanism suggested in a conceptual model by Velo-Suárez et al (2009) to explain the persistence of *D. acuminata* in the Galician Rías Baixas.

Most of the *D. acuminata* population remained in the top 5 m of the water column, at least throughout the 36-h sampling, and showed little evidence of vertical migration. But detection of cell maxima at 10 m in some profiles sampled at midnight before the cruise (see Fig. 3B) suggests that this was not always the case. In contrast, its ciliate prey

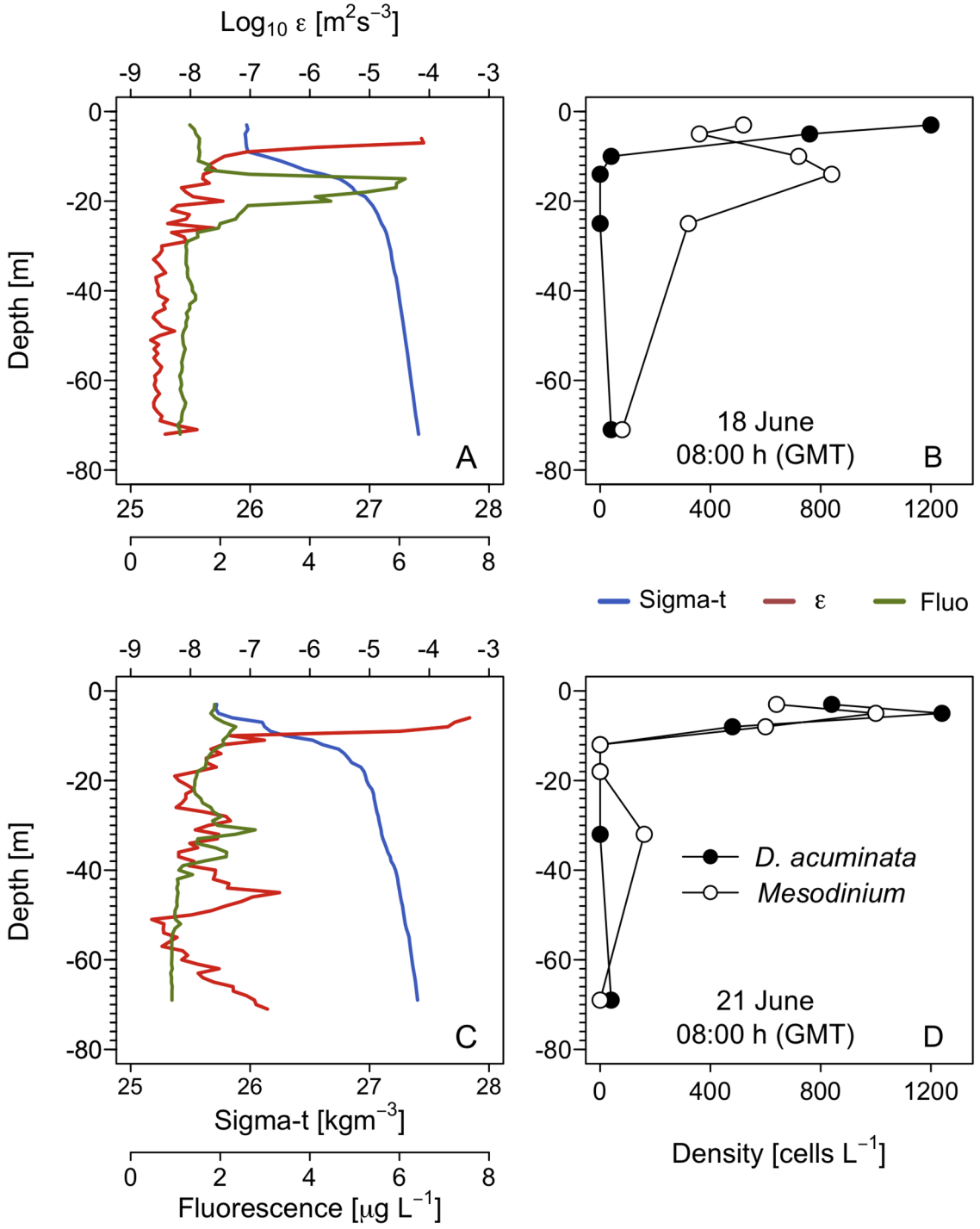


**Fig. 10.** Vertical profiles on a shelf station (V5) off Ría de Vigo: (A, C) Vertical distribution of density, in vivo fluorescence and turbulent kinetic energy dissipation rate ($\varepsilon$) and (B, D) Vertical distribution of *Dinophysis acuminata* and *Mesodinium* cells (cells $L^{-1}$) on June 18 and 21, 2013 at 08:00 GMT.

maxima appeared below the pycnocline at night and nearer the surface in the afternoon. We must be cautious about interpreting this distribution as vertical migration, because sampling was carried out at a fixed station, but there is a body of literature about the swimming behaviour of *Mesodinium* and its daily vertical migration (Crawford and Lindholm, 1997; Lindholm, 1985). Thus, populations of *Dinophysis* and its ciliate prey co-occurred in time, but they only overlapped when the ciliate prey aggregated near the surface after noon. These observations agree with the scenario reported by Sjöqvist and Lindholm (2011) in a stratified coastal inlet in the Northern Baltic Sea. These authors described the vertical migration of *Mesodinium*, descending at night to nutrient richer waters and ascending in the morning. *D. acuminata* did not perform vertical diurnal migration in the Baltic Sea but its maxima overlapped with those of *Mesodinium* at noon hours. There is also agreement with the observations from González-Gil et al. (2010) during a 14 d cruise from June 1 to 14 and a 24 h cycle study, both in the same area, the Ria de Pontevedra. These authors reported that patches of *D. acuminata* and *Mesodinium* moved around the ría, and only occasionally met. When the two populations coincided, *D. acuminata* did not exhibit daily vertical migration (DVM) during a 24 h sampling during downwelling. In contrast, *Mesodinium* appeared aggregated at the surface at 06.30 and 17.00, and evenly distributed in the top 8 m layer the rest of

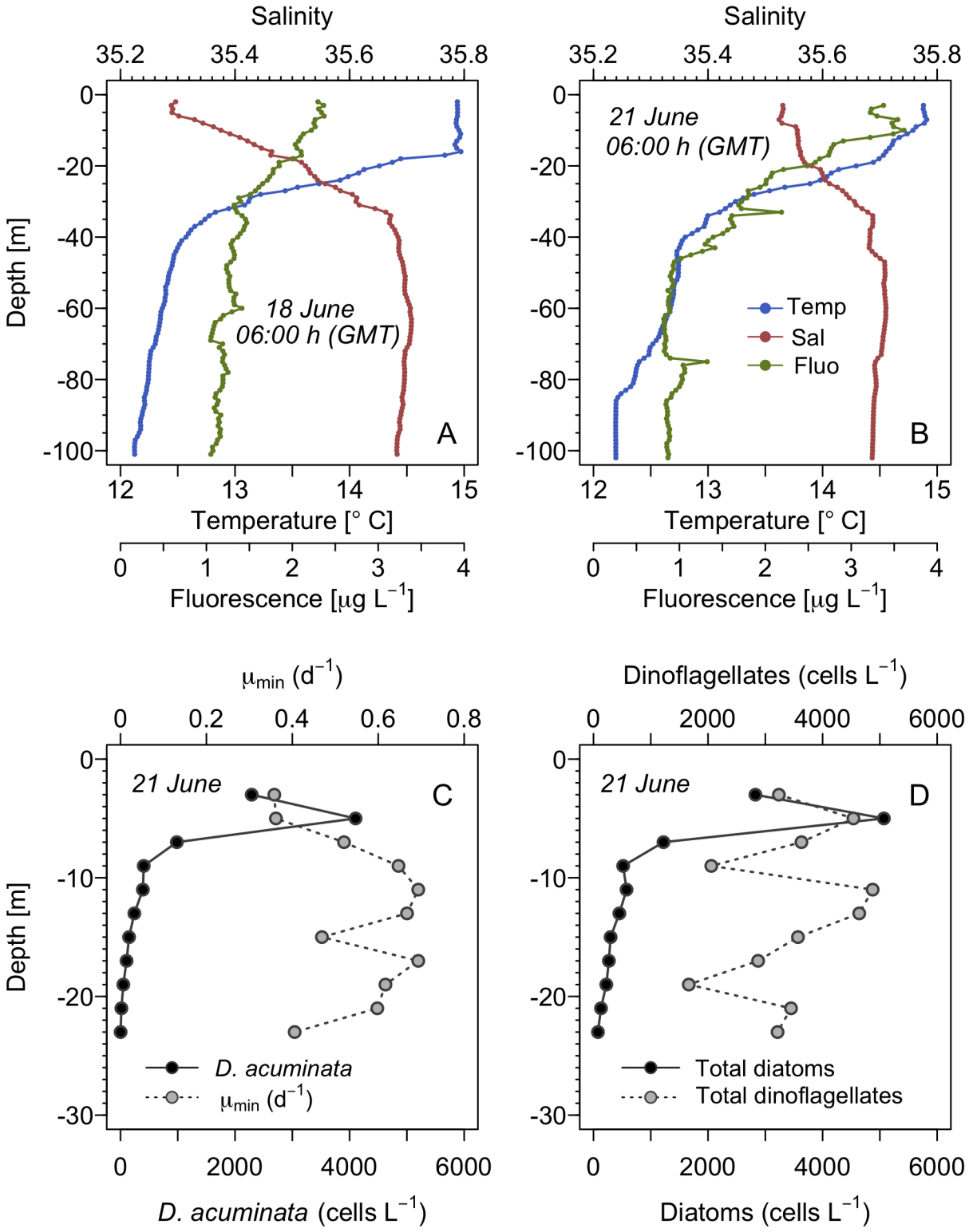


**Fig. 11.** Vertical profiles on a shelf station (V6) off Ría de Vigo. (A-B) Vertical distribution of temperature, salinity and in vivo fluorescence on 18 and 21 June at 06:00 GMT. (C) Vertical distribution of *Dinophysis acuminata* (cells $L^{-1}$) and $\mu_{min}$, and of (D) Total densities of diatoms and dinoflagellates (cells $L^{-1}$) on June 21, 2013.

the time. The two populations appeared to have distinct niches and distinct responses to physical forcing. In contrast, Villarino et al. (1995) reported that *D. acuminata* and *Mesodinium* performed a similar DVM pattern in Ría de Vigo. The fact that their sampling took place at the end of summer (19–20 September 1991) under very calm weather and strong thermal stratification (4.5 °C gradient between the surface and 9 m depth) may explain the different behaviour of the dinoflagellate and its ciliate prey. These observations support the view that *Dinophysis* behaviour varies depending on the nutritional status and phase of the population growth (Reguera et al., 2012). But our observations in previous studies and here suggest a possible "ambush" strategy of *Dinophysis* to catch its fast swimming ciliate prey: to remain the whole day

at a fixed depth and intercept the ciliates as they ascend.

Physiological studies with *D. acuminata* and *M. rubrum* cultures shed new light on their behavioural differences. Both species are kleptoplastidic mixotrophs, but carbon uptake from live prey in *Mesodinium* represents only about 2% of its daily intake, whereas it is 50% in the case of *Dinophysis acuminata* (reviewed by Hansen et al., 2013). Thus, *D. acuminata* may grow in nutrient-poor surface waters provided it has ciliate prey, but *Mesodinium* will be more dependent on resources from nutrient-rich layers, in or below the pycnocline, visited during DVM at night, and light for photosynthesis at midday. Of special interest are other plastid-bearing ciliates which co-occured with *D. acuminata* in this study. Plastid-retaining oligotrichous ciliates (e.g. *Cyrtostrombidium*, *Laboea*, *Strombidium* and *Tontonia*) might provide alternative prey for growth of *Dinophysis* species provided they retain plastids of suitable cryptophyte species (Stoecker et al., 2009). So far, only cryptophyte plastids belonging to the *Tetraselmis/Plagioselmis/Geminigera* (TPG) clade have been regularly found in field specimens of *Dinophysis* species (Reguera et al., 2012). Over 90% of the plastids sequenced from *Dinophysis*, mainly *D. acuminata*, in the Galician Rías had a difference of just 1 bp from those of *Teleaulax amphioxeia* (Rial et al., 2015). Nevertheless, plastids from more species and strains of *Dinophysis* and from more mixotrophic ciliates need to be analyzed as potential alternative prey to *Mesodinium*.

### 4.3. Changes in division-rates (μ) in D. acuminata populations during the transition from relaxation to upwelling

The post-mitotic index method applied in this study is a simple and reliable way to estimate *in situ* division rates of *Dinophysis* species representing a small fraction of the microplankton community. This method has been applied in several previous studies in the Galician Rías, and has provided background information on the cell-cycle behaviour of different species of *Dinophysis*, including their specific time-window for synchronized or in-phase division (Reguera et al., 2003; Pizarro et al., 2008; Velo-Suárez et al., 2008, 2009). Estimates of *in situ* division rates ($\mu_{avg}$) of *Dinophysis* spp. in previous studies have shown large variability related to the population growth phase and to changing environmental conditions. Almost nil division rates ($0.09\ d^{-1}$) were observed during the stationary phase of a *D. acuminata* population in the same area and time of year (mid-June 1998) (Reguera et al., 2003) and in a *D. acuta* population with a sharp increase in net growth associated with physical accumulation of stationary-phase shelf populations (Escalera et al., 2010). In contrast, high rates close to one division per day ($\mu = 0.6\ d^{-1}$), presumably triggered by a recent encounter and feeding on a *Mesodinium* patch, were observed in June 2005 (González-Gil et al., 2010; Velo-Suárez et al., 2014). Velo-Suárez et al. (2009) showed that during late spring relaxation, increased densities of *D. acuminata* inside the rías resulted from physical advection combined with high *in situ* growth.

The opposite scenario is described in the present study at the onset of an upwelling pulse near neap tide. Decreased densities of a *D. acuminata* population resulted from a combination of physical dispersion and accompanying decline of *in situ* ($\mu_{avg}$) growth. Upwelling-induced transport of the toxic dinoflagellate *Gymnodinium catenatum* and other harmful microalgae off the Galician Rías Baixas (Fermin et al., 1996), and the reset of the phytoplankton succession and rapid development of diatom-dominated assemblages of colonizers following upwelling pulses (Nogueira and Figueiras, 2005; Tilstone et al., 2000) are well documented. Upwelling pulses lead to increased flushing rates of surface waters (Álvarez-Salgado et al., 1993). During the first stages of a relaxation-upwelling transition, increased outflows lead to a remarkable decrease of planktonic populations before a new diatom bloom is triggered (Varela et al., 2008). Increased shear stress in the pycnocline region and higher horizontal water velocities in the top layer have been recorded even during moderate upwelling pulses (Velo-Suárez et al., 2010). ADCP records in the present study provide strong evidence of increased surface outflow between 17 and 19 June (Fig. 5).

A different matter is the direct negative effect (reduced division rate) that the onset of an upwelling pulse and increased turbulence may have on the physiology of *D. acuminata*. The effect of microscale turbulence in altering or even bringing to a halt cellular division (Berdalet, 1992; Juhl and Latz, 2002; Sullivan et al., 2003; Berdalet et al., 2007), motility, sexual processes, cell shape (Berdalet and Estrada, 1995; Zirbel et al., 2000) and the transport of substances in and out of the cells (Karp-Boss et al., 1996) in dinoflagellates is well documented. In the present study, the division rate of a very fit population of *D. acuminata* ($\mu_{avg} = 0.65\ d^{-1}$, almost one doubling per day) was halved (to $0.33\ d^{-1}$) in 24 h following the onset of upwelling 2 days before and the shoaling of colder, nutrient richer upwelling waters at an estimated rate of $0.33\ m\ h^{-1}$. Further, the circadian rhythm (maximum division at dawn) was altered, and the shape of the frequency distribution curves evolved from an acute-, indicating more synchronized division, to a wider and flatter dome. Upwelled waters may contribute to increase phytoplankton cell densities by shoaling pycnoclines and bringing cells closer to the well illuminated surface layer. This was not the case in the population studied here, because *D. acuminata* cell maxima were already in the top layer before the upwelling pulse, and they remained in this layer throughout the 36-h cycle. The onset of northerly winds could have at least two effects on the near-surface layer: increased turbulence and increased flushing, as well as the upwelling itself. ADCP and turbulence profiler data from the top 3 m are not reliable due to side lobe effects. Nevertheless, turbulence profiles provided evidence of changes of $\varepsilon$ over two orders of magnitude (from $10^{-6}$ to $10^{-4}\ m^2\ s^{-3}$) at 5 m during several time windows in the cell cycle (Fig. 4E). It is true that turbulence increased before division time in the first cycle, on June 19 at dawn, but division one day tends to reflect the previous 24 h life history of the cells and in any case, northerly winds intensification started on June 18 (Fig. 2B).

There is hardly any information available on the effect of microscale turbulence on *Dinophysis* division, but a recent study by García-Portela (2018) with *D. acuminata* cultures exposed to different levels of turbulence with an oscillating grid showed very poor growth under high turbulence ($\varepsilon = 10^{-4}$–$10^{-3}\ m^2\ s^{-3}$) compared with lower values ($\varepsilon = 10^{-6}$–$10^{-5}\ m^2\ s^{-3}$). In addition, upwelled waters cause cooling of the surface layer, which in the present study was from 16.84 °C to 14.67° at 5 m, from 20:00 h on June 19 to 04:00 h on June 20, i.e., more than 2 °C drop in only 8 h.

Our results suggest that downwelling-upwelling transitions within the rías have a double effect, both contributing to decreased cell densities in established populations of *D. acuminata*: a direct physical effect of advective dispersion, and a physiological stress inflicted on the cells by the rapid rising of turbulence and cooling of surface waters.

Mid-shelf (100 m isobath) surface water conditions did not show such marked changes as those inside the rías, where shoaling of isoclines during upwelling and sinking during downwelling created contrasting short-lived vertical structures. Fig. 3 shows that on June 18, when the top 15–20 m were homogeneous, there was a conspicuous stratification at the mid-shelf stations that was not completely eroded after the upwelling pulse (Figs. 10C, 11B). Further, temperature in the top layer (~15 °C) did not show significant changes, and division rates ($\mu_{min}$) at the surface cell maximum at station V6 ($0.36\ d^{-1}$) were as high as those inside the ría before the upwelling event. But the most surprising observation was the extremely fit condition ($\mu_{min} = 0.69$) of the low density population in the subsurface layer (10–18 m) at this station on June 21. The value of $\mu_{min}$ there indicates that the whole population had gone through mitosis, and all cells could be recognized as recently-divided specimens in a single sample at peak division hour (06:00 h, dawn), i.e. they were perfectly synchronized, whereas populations inside the ría divided in-phase, i.e., all cells going through mitosis were doing so within a discrete time window. These observations suggest that when *Dinophysis* and other dinoflagellate species are transported out of the rías to mid-shelf waters during upwelling pulses, this region

(upwelling front) will act as the pelagic seed bank (sensu Smayda, 2002) where cells will aggregate and keep in good condition (high division rates) until the next relaxation period re-introduces them into the rías. Several facts support this view. First, upwelling fronts in shelf waters have been described as horizontal retention areas where good planktonic swimmers can aggregate (Smayda, 2010a; Smayda, 2010b). In addition, upwelling fronts have been identified as important horizontal limits for the distribution of *Gymnodinium catenatum* and *Dinophysis* species in Portuguese shelf waters (Moita, 1993; Moita et al., 1998), and as the "incubator" of inoculum populations of *Dinophysis acuta* before they are transported to shellfish cultivation areas in SW Ireland (Raine et al., 2016).

Changes of toxin (OA) accumulation per cell throughout the two cell cycles did not show any clear circadian pattern. The "normal" expected result would have been a decline in toxin per cell at 06.00 on June 19 coinciding with the peak in recently divided cells. Nevertheless, toxin per cell estimates from net-haul samples may be noisy due to contamination with other species. Results are reliable when there is an overwhelming dominance of the target organism in the net-haul material, as is often the case during downwelling (Reguera et al., 2011, 2014). But in the present study, samples had variable amounts of the predominant diatoms.

### 4.4. Concluding remarks

High resolution vertical sampling at a fixed station in Ría de Pontevedra (Galician Rías, NW Spain) showed physical processes (upwelling pulse, changes in turbulence) associated with the shoaling, erosion and renewal of a diatom thin layer. A co-occurring population of *Dinophysis acuminata* had its cell maxima at the surface throughout a 36 h cell cycle study, with no evidence of daily vertical migration. In contrast, its ciliate prey (*Mesodinium* spp.) maxima were below the pycnocline at night and near the surface in the afternoon, when they coincided with the dinoflagellate maximum. Other mixotrophic ciliates with similar behaviour to *Mesodinium* also co-occurred with *D. acuminata*. Their potential role as alternative prey for *Dinophysis* deserves investigation.

The onset of upwelling pulses and associated increase of surface outflow caused advective dispersion of phytoplankton populations, in particular of *Dinophysis,* and a rapid cooling of the surface layer where the latter was distributed. In addition, the northerly winds increase turbulence directly, maximaly at the surface. Therefore, the onset of upwelling pulses and the intensified northerly winds promoting them will cause a decline in the population growth of *Dinophysis* due to: i) a direct physical effect of advective dispersion favouring the transport of cells in the surface layer of the rías to shelf waters, and ii) an indirect effect of physiological disturbance of the cells, mainly through enhanced turbulence and rapid temperature drop in the surface layer, leading to reduced division rates. At the same time, shelf conditions are more stable, with a moderate decline of surface temperature, and relatively similar levels of turbulence in the upper 30 m before and after the upwelling pulse. Shelf populations of *Dinophysis* seemed relatively undisturbed, showing division rates comparable to those of the populations in the ría before the onset of upwelling. These shelf populations may act as a reservoir for subsequent bloom formation.

## Acknowledgements

We thank I. Ramilo, P. Rial and G. Fernández for technical assistance during the *ASIMUTH-Rías 2013* cruise and phytoplankton counts. This work and the sampling cruise were funded by project ASIMUTH (EC FP7-SPACE-2010-1 grant agreement number 261860). Additional support came from Spanish project REMEDIOS (MINECO, Programa RETOS, CTM2016-75451-C2-2-R), and the EU Interreg Atlantic Area PRIMROSE (EAPA_182/2016), an IOC-SCOR GlobalHAB endorsed project. Patricio A. Díaz had a PhD student fellowship from BECAS–CHILE, National Commission for Scientific and Technological Research (CONICYT) and is now funded by projects PAI79160065 (The Attraction and Insertion of Advanced Human Capital Program) and REDES170101 (International Cooperation Programme), CONICYT, Chile.

## References

Aissaoui, A., Dhib, A., Reguera, R., Ben Hassine, O.K., Turki, S., Aleya, L., 2014. First evidence of cell deformation occurrence during a *Dinophysis* bloom along the shores of the Gulf of Tunis (SW Mediterranean Sea). Harmful Algae 39, 191–201.

Álvarez-Salgado, X.A., Figueiras, F.G., Pérez, F.F., Groom, S., Nogueira, E., Borges, A.V., Chou, L., Castro, C.G., Moncoiffé, G., Ríos, A.F., Miller, A.E., Frankignoulle, M., Savidge, G., Wollast, R., 2003. The Portugal coastal counter current off NW Spain: new insights on its biogeochemical variability. Prog. Oceanogr. 56, 281–321.

Álvarez-Salgado, X.A., Rosón, G., Pérez, F.F., Pazos, Y., 1993. Hydrographic variability off the Rías Baixas (NW Spain) during the upwelling season. J. Geophys. Res. 98, 14447–14455.

Bakun, A., 1973. Coastal Upwelling Indices, West Coast of North America, 1946-71. U.S. Dep. Commer., NOAA Technical Report, NMFS SSRF-671.

Bakun, A., Nelson, A., 1991. The seasonal cycle of wind stress curl in subtropical eastern boundary current regions. J. Phys. Oceanogr. 21, 1815–1834.

Berdalet, E., 1992. Effects of turbulence on the marine dinoflagellate *Gymnodinium nelsonii*. J. Phycol. 28, 267–272.

Berdalet, E., Estrada, M., 1995. Effects of turbulence on several phytoplankton species. In: Smayda, T.J., Shimizu, Y. (Eds.), Toxic Phytoplankton Blooms in the Sea. Developments in Marine Biology, 5th International Conference on Toxic Marine Phytoplankton, Rhode Island, USA. Elsevier, New York, USA, pp. 737–740.

Berdalet, E., Peters, F., Koumandou, V., Roldán, C., Guadayol, O., Estrada, M., 2007. Species-specific physiological response of dinoflagellates to quantified small-scale turbulence. J. Phycol. 43, 965–977.

Blanco, J., Moroño, A., Fernández, M.L., 2005. Toxic episodes in shellfish produced by lipophilic phycotoxins: an overview. Galician J. Mar. Resour. 1, 70.

Blanco, J., Correa, J., Muñíz, S., Mariño, C., Martín, H., Arévalo, F., 2013. Evaluación del impacto de los métodos y niveles utilizados para el control de toxinas en el mejillón. Revista Galega dos Recursos Mariños 3, 1–55.

Carpenter, E.J., Chang, J., 1988. Species-specific phytoplankton growth rates via diel DNA synthesis cycles. I. Concept of the method. Mar. Ecol. Prog. Ser. 43, 105–111.

Chang, J., Carpenter, E.J., 1991. Species-specific phytoplankton growth rates via diel DNA synthesis cycles. V. Application to natural populations. Mar. Ecol. Prog. Ser. 78, 115–122.

Crawford, D.W., Lindholm, T., 1997. Some observations on vertical distribution and migration of the phototrophic ciliate *Mesodinium rubrum* (=*Myrionecta rubra*) in a stratified brackish inlet. Aquat. Microb. Ecol. 13, 267–274.

Díaz, P.A., Reguera, B., Ruiz-Villarreal, M., Pazos, Y., Velo-Suárez, L., Berger, H., Sourisseau, M., 2013. Climate variability and oceanographic settings associated with interannual variability in the initiation of *Dinophysis acuminata* blooms. Mar. Drugs 11, 2964–2981.

Díaz, P.A., Ruiz-Villarreal, M., Velo-Suárez, L., Ramilo, I., Gentien, P., Lunven, M., Fernand, L., Raine, R., Reguera, B., 2014. Tidal and wind-event variability and the distribution of two groups of *Pseudo-nitzschia* species in an upwelling-influenced Ría. Deep Sea Res. II 101, 163–179.

Díaz, P.A., Ruiz-Villarreal, M., Pazos, Y., Moita, M.T., Reguera, B., 2016. Climate variability and *Dinophysis acuta* blooms in an upwelling system. Harmful Algae 53, 145–159.

Escalera, L., Reguera, B., Moita, T., Pazos, Y., Cerejo, M., Cabanas, J.M., Ruiz-Villarreal, M., 2010. Bloom dynamics of *Dinophysis acuta* in an upwelling system: *In situ* growth versus transport. Harmful Algae 9, 312–322.

Farrell, H., Velo-Suárez, L., Reguera, B., Raine, R., 2014. Phased cell division, specific division rates and other biological observations of *Dinophysis* populations in subsurface layers off the south coast of Ireland. Deep Sea Res. II 101, 249–254.

Fermin, E.G., Figueiras, F.G., Arbones, B., Villarino, M.L., 1996. Short-time scale development of a *Gymnodinium catenatum* population in the Ria de Vigo (NW Spain). J. Phycol. 32, 212–221.

Fernández-Castro, B., Mouriño-Carballido, B., Benítez-Barrios, V.M., Chouciño, P., Fraile-Nuez, E., Graña, R., Piedeleu, M., Rodríguez-Santana, A., 2014. Microstructure turbulence and diffusivity parameterization in the tropical and subtropical Atlantic, Pacific and Indian Oceans during the Malaspina 2010 expedition. Deep Sea Res. I 94, 15–30.

Fernández-Castro, B., Gilcoto, M., Naveira-Garabato, A., Villamaña, M., Graña, R., Mouriño-Carballido, B., 2018. Modulation of the semidiurnal cycle of turbulent dissipation by wind-driven upwelling in a coastal embayment. J. Geophys. Res. 123. https://doi.org/10.1002/2017JC013582.

Figueiras, F.G., Ríos, A.F., 1993. Phytoplankton succession, red tides and the hydrographic regime in the Rias Bajas of Galicia. In: Smayda, T.J., Shimizu, Y. (Eds.), Toxic Phytoplankton Blooms in the Sea. Developments in Marine Biology, 5th International Conference on Toxic Marine Phytoplankton, Rhode Island, USA. Elsevier, New York, USA, pp. 239–244.

Garcés, E., Delgado, M., Camp, J., 1997. Phased cell division in a natural population of *Dinophysis sacculus* and the *in situ* measurement of potential growth rate. J. Plankton Res. 19, 2067–2077.

García-Portela, M., 2018. Comparative ecophysiology of two mixotrophic species of *Dinophysis* producers of lipophilic toxins. PhD Thesis, Universidad de Vigo, 2018.

GEOHAB, 2005. Global Ecology and Oceanography of Harmful Algal Blooms. In: Pitcher, G., Moita, T., Trainer, V., Kudela, R., Figueiras, F., Probyn, T. (Eds.) IOC and SCOR, GEOHAB Core Research Project: HABs in Upwelling Systems. Paris and Baltimore, 88.

Gibson, C.H., Thomas, W.H., 1995. Effects of turbulence intermittency on growth inhibition of a red tide dinoflagellate, *Gonyaulax polyedra* Stein. J. Geophys. Res. 100, 24841–24846.

Gilcoto, M., Largier, J.L.D., Barton, E.D., Piedracoba, S., Torres, R., Graña, R., Alonso-Pérez, F., Villacieros-Robineau, N., de la Granda, F., 2017. Rapid response to coastal upwelling in a semienclosed bay. Geophys. Res. Lett. https://doi.org/10.1002/2016GL072416.

González-Gil, S., Velo-Suárez, L., Gentien, P., Ramilo, I., Reguera, R., 2010. Phytoplankton assemblages and characterization of a *Dinophysis acuminata* population during an upwelling-downwelling cycle. Aquat. Microb. Ecol. 58, 273–286.

Hansen, P.J., Nielsen, L.T., Johnson, M., Berge, T., Flynn, K.J., 2013. Acquired phototrophy in *Mesodinium* and *Dinophysis* – A review of cellular organization, prey selectivity, nutrient uptake and bioenergetics. Harmful Algae 28, 126–139.

Kim, S., Kang, Y.G., Kim, H.S., Yih, W., Coats, D.W., Park, M.G., 2008. Growth and grazing responses of the mixotrophic dinoflagellate *Dinophysis acuminata* as functions of light intensity and prey concentration. Aquat. Microb. Ecol. 51, 301–310.

Juhl, A., Latz, M., 2002. Mechanisms of fluid shear-induced inhibition of population growth in a red-tide dinoflagellate. J. Phycol. 38, 683–694.

Karp-Boss, L., Boss, E., Jumars, P.A., 1996. Nutrient fluxes to planktonic osmotrophs in the presence of fluid motion. Oceanogr. Mar. Biol. Annu. Rev. 34, 71–109.

Lasker, R., 1978. The relation between oceanographic conditions and larval anchovy food in the California current: factors leading to recruitment failure. Rapp. P.-V. Reun. Cons. int. Explor. Mer. 173, 212–230.

Lindholm, T., 1985. *Mesodinium rubrum* – a unique photosynthetic ciliate. Adv. Aquatic Microbiol. 8, 1–48.

Lynn, D.H., Small, E.B., 2002. Phylum Ciliophora Doflein, 1901. In: Lee, J.J., Leedale, G. F., Bradbury, P. (Eds.), An Illustrated Guide to the Protozoa, Vol. 1 Allen Press, Lawrence, USA, pp. 371–656.

Margalef, R., 1978. Life forms of phytoplankton as survival alternatives in an unstable environment. Oceanol. Acta 1, 493–509.

Margalef, R., Estrada, M., Blasco, D., 1979. Functional morphology of organisms involved in red tides, as adapted to decaying turbulence. In: Taylor, D., Seliger, H. (Eds.), Toxic Dinoflagellate Blooms. Elsevier, New York, pp. 89–94.

McDuff, R.E., Chisholm, S.W., 1982. The calculation of *in situ* growth rates of phytoplankton populations from fractions of cells undergoing mitosis: a clarification. Limnol. Oceanogr. 27, 783–788.

Moita, M.T., 1993. Development of toxic dinoflagellates in relation to upwelling patterns off Potugal. In: Smayda, T.J., Shimizu, Y. (Eds.), Toxic Phytoplankton Blooms in the Sea. Developments in Marine Biology, 5th International Conference on Toxic Marine Phytoplankton, Rhode Island, USA. Elsevier, New York, USA, pp. 299–304.

Moita, M.T., Vilarinho, M.G., Palma, A.S., 1998. On the variability of Gymnodinium catenatum Graham blooms in Portuguese waters. In: Reguera, B. Blanco, J., Fernández, M.L., Wyatt, T. (Eds.), Harmful Algae. Xunta de Galicia and IOC of UNESCO, Santiago de Compostela, Spain, pp. 118–121.

Moita, M.T., Silva, A.J., 2001. Dynamics of *Dinophysis acuta*, *D. acuminata*, *D. tripos* and *Gymnodinium catenatum* during an upwelling event off the Northwest Coast of Portugal. In: Hallegraeff, G.M., Blackburn, S.I., Bolch, C.J., Lewis, R.J. (Eds.), Harmful Algal Blooms 2000. Intergovernmental Oceanographic Commission of UNESCO, Paris, pp. 169–172.

Nogueira, E., Figueiras, F.G., 2005. The microplankton succession in the Ría de Vigo revisited: Species assemblages and the role of weather-induced, hydrodynamic variability. J. Mar. Syst. 54, 139–155. https://doi.org/10.1016/j.jmarsys.2004.07.

Otero, P., Ruiz-Villarreal, M., Garcia-Garcia, L., Gonzalez-Nuevo, G., Cabanas, J.M., 2013. Coastal dynamics off Northwest Iberia during a stormy winter period. Ocean Dyn. 63, 115–129.

Park, M., Kim, S., Kim, H., Myung, G., Kang, Y., Yih, W., 2006. First successful culture of the marine dinoflagellate *Dinophysis acuminata*. Aquat. Microb. Ecol. 45, 101–106.

Pizarro, G., Escalera, L., González-Gil, S., Franco, J., Reguera, B., 2008. Growth, behaviour and cell toxin quota of *Dinophisis acuta* during a daily cycle. Mar. Ecol. Prog. Ser. 353, 89–105.

Prandke, H., Stips, A., 1998. Test measurements with an operational microstructure-turbulence profiler: Detection limit of dissipation rates. Aquat. Sci. 60, 191–2009.

Prandke, H., Holtsch, K., Stips, A., 2000. MITEC Technology Development: The Microstructure/Turbulence Measuring System MSS. Space Applications Institute, Ispra.

Raine, R., Cosgrove, S., Fennell, S., Gregory, C., Bernett, M., Purdie, D., Cave, R., 2016. Origins of *Dinophysis* blooms which impact Irish aquaculture. In: Anonymous, International Conference on Harmful Algae. Florianópolis, Brazil: 9-14 October 2016, Book of Abstracts pp. 57.

Reguera, B., Garcés, E., Pazos, Y., Bravo, I., Ramilo, I., González-Gil, S., 2003. Cell cycle patterns and estimates of *in situ* división rates of dinoflagellates of the genus *Dinophysis* by a postmitotic index. Mar. Ecol. Prog. Ser. 249, 117–131.

Reguera, B., Riobó, P., Rodríguez, F., Díaz, P.A., Pizarro, G., Paz, B., Franco, J.M., Blanco, J., 2014. *Dinophysis* toxins: causative organisms, distribution and fate in shellfish. Mar. Drugs 12, 394–461.

Reguera, B., Rodríguez, F., Blanco, J. 2011. Harmful algae blooms and food safety: physiological and environmental factors affecting toxin production and their accumulation in shellfish. In: Cabado, A.G, Vieites, J.M. (Eds) New Trends in Marin and Freshwater Toxins: Food Safety Concerns. Chapter 3. Nova Science Publishers, In., New York, USA.

Reguera, B., Velo-Suárez, L., Raine, R., Park, M., 2012. Harmful *Dinophysis* species: A review. Harmful Algae 14, 87–106.

Rial, P., Garrido, J.L., Gaen, D.R., Rodríguez, F., 2015. Exploring the origin of cryptophyte plastids in *Dinophysis* from Galician waters: results from field and culture experiments. J. Plankon Res. 35 (2), 433–437.

Ruiz-Villarreal, M., García-García, L., Cobas, M., Díaz, P.A., Reguera, B., 2016. Modelling the hydrodynamic conditions associated with *Dinophysis* blooms in Galicia (NW Spain). Harmful Algae 53, 40–52.

Sjöqvist, C.O., Lindholm, T.J., 2011. Natural co-occurrence of *Dinophysis acuminata* (Dinoflagellata) and *Mesodinium rubrum* (Ciliophora) in thin layers in a coastal inlet. J. Eukaryot. Microbiol. 58, 365–372.

Smayda, T., 2002. Turbulence, watermass stratification and harmful algal blooms: an alternative view and frontal zones as "pelagic seed banks". Harmful Algae 1, 95–112.

Smayda, T., 2010a. Adaptations and selection of harmful and other dinoflagellate species in upwelling systems 1. Morphology and adaptive polymorphism. Prog. Oceanogr. 85, 53–70.

Smayda, T., 2010b. Adaptations and selection of harmful and other dinoflagellate species in upwelling systems. 2. Motility and migratory behaviour. Prog. Oceanogr. 85, 71–91.

Smayda, T., Reynolds, C., 2001. Community assembly in marine phytoplankton: application ofrecent models to harmful dinoflagellate blooms. J. Plankton Res. 23, 447–461.

Stoecker, D.K., Johnson, M.D., de Vargas, C., Not, F., 2009. Acquired phototrophy in aquatic protists. Aquat. Microb. Ecol. 57, 279–310.

Sullivan, J., Swift, E., Donaghay, P., Rines, J., 2003. Small-scale turbulence affects the division rate and morphology of two red-tide dinoflagellates. Harmful Algae 2, 183–199.

Thomas, W., Gibson, C., 1990a. Effects of small-scale turbulence on microalgae. J. Appl. Phycol. 2, 71–77.

Thomas, W., Gibson, C., 1990b. Quatified small-scale turbulence inhibits a red tide dinoflagellate, *Gonyaulax polyedra* Stein. Deep-Sea Res. 37, 1583–1593.

Thomas, W., Vernet, M., Gibson, C., 1995. Effects of small-scale turbulence on photosynthesis, pigmentation, cell division, and cell size in the marine dinoflagellate *Gonyaulax polyedra* (Dinophyceae). J. Phycol. 31, 50–59.

Tilstone, G.H., Míguez, B.M., Figueiras, F.G., Fermín, E.G., 2000. Diatom dynamics in a coastal ecosystem affected by upwelling: coupling between species succession, circulation and biogeochemical processes. Mar. Ecol. Prog. Ser. 205, 23–41.

Utermöhl, H., 1958. Zur Vervollkomnung der quantitativen phytoplankton-Methodik. Mitteilungen – Internationale Vereinigung für Theoretische und Angewandte Limnologie 9, 1–38.

Varela, M., Prego, R., Pazos, Y., 2008. Spatial and temporal variability of phytoplankton biomass, primary production and community structure in the Pontevedra Ria (NW Iberian Peninsula): oceanographic periods and possible response to environmental changes. Mar. Biol. 154, 483–499.

Velo-Suárez, L., González-Gil, S., Gentien, P., Lunven, M., Bechemin, C., Fernand, L., Raine, R., Reguera, B., 2008. Thin layers of *Pseudo-nitzschia* spp. and the fate of *Dinophysis acuminata* during an upwelling–downwelling cycle in a Galician Ría. Limnol. Oceanogr. 53, 1816–1834.

Velo-Suárez, L., Fernand, L., Gentien, P., Reguera, B., 2010. Hydrodynamic conditions associated with the formation, maintenance and dissipation of a phytoplankton thin layer in a coastal upwelling system. Cont. Shelf Res. 30, 193–202.

Velo-Suárez, L., González-Gil, S., Pazos, Y., Reguera, B., 2014. The growth season of *Dinophysis acuminata* in an upwelling system embayment: A conceptual model based on *in situ* measurements. Deep Sea Res. II 101, 141–151.

Velo-Suárez, L., Reguera, B., Garcés, E., Wyatt, T., 2009. Vertical distribution of division rates in coastal dinoflagellate *Dinophysis* spp. populations: implications for modelling. Mar. Ecol. Prog. Ser. 385, 87–96.

Villamaña, M., Mouriño-Carballido, B., Marañón, E., Cermeño, P., Chouciño, P., da Silva, J.C.B., Díaz, P.A., Fernández-Castro, B., Gilcoto, M., Graña, R., Latasa, M., Magalhaes, J.M., Luis Otero-Ferrer, J., Reguera, B., Scharek, R., 2017. Role of internal waves on mixing, nutrient supply and phytoplankton community structure during spring and neap tides in the upwelling ecosystem of Ría de Vigo (NW Iberian Peninsula). Limnol. Oceanogr. 62, 1014–1030.

Villarino, M.L., Figueiras, F., Jones, K., Alvarez-Salgado, X.A., Richard, J., Edwards, A., 1995. Evidence of *in situ* diel vertical migration of a red-tide microplancton species in Ría de Vigo (NW Spain). Mar. Biol. 123, 607–617.

Wyatt, T., 2014. Margalef's mandala and phytoplankton bloom strategies. Deep Sea Res. II 101, 32–49.

Zirbel, M.J., Veron, F., Latz, M.I., 2000. The reversible effect of flow on the morphology of *Ceratium horrida* (Peridiniales, Dinophyta). J. Phycol. 36, 46–58.